

Calculations of the Exclusive Processes $^2\text{H}(e, e'p)n$, $^3\text{He}(e, e'p)^2\text{H}$ and $^3\text{He}(e, e'p)(pn)$ within a Generalized Glauber Approach

C.Ciofi degli Atti and L.P. Kaptari*

*Department of Physics, University of Perugia and Istituto Nazionale di Fisica Nucleare,
Sezione di Perugia, Via A. Pascoli, I-06123, Italy*

(Dated: May 23, 2019)

Abstract

The exclusive processes $^2H(e, e'p)n$, $^3He(e, e'p)^2H$ and $^3He(e, e'p)(pn)$, have been analyzed using realistic few-body wave functions and treating final state interaction (FSI) effects within a Generalized Glauber approach (GGA), based on the direct calculation of the Feynman diagrams which describe the rescattering of the struck nucleon with the nucleons of the $A - 1$ system. The approach represents an improvement of the conventional Glauber eikonal approach (GA) where it is assumed that: i) target nucleons are stationary during the multiple scattering of the struck nucleon with the nucleons of the spectator system $A - 1$ (the *frozen approximation*), and ii) only perpendicular momentum transfer components are considered in nucleon-nucleon (NN) rescattering. The GGA, originally developed by various authors in different contexts, takes into account the effects of the nuclear excitation of the $A - 1$ system, which leads to a dependence of the profile function upon the removal energy of the struck nucleon and, consequently, to a variation of the longitudinal component of the missing momentum; thus, in the GGA the effects of the Fermi motion of the $A - 1$ system on the rescattering of the struck nucleon is taken into account, and the frozen approximation is removed. The basic elements of the GGA method are presented and a relevant related topic, namely the factorization of the cross section for the exclusive process $A(e, e'p)B$ frequently adopted in the calculations, is discussed within the context of the GA and GGA approximation. Our approach is a very transparent one and fully parameter free: realistic wave functions resulting from few-body calculations are used and FSI effects are fixed by NN scattering data. The available experimental data on the processes $^2H(e, e'p)n$, $^3He(e, e'p)^2H$, and $^3He(e, e'p)(pn)$, are compared with theoretical predictions obtained within both the GA and the GGA, and a general good agreement is obtained for both the two- and the three-body systems. It is found that in some kinematical conditions FSI effects represent small corrections, whereas in other kinematics conditions they are very large and absolutely necessary to provide a satisfactory agreement between theoretical calculations and experimental data. It is shown that in the kinematics of the experimental data which have been considered, covering a region of missing momentum and energy $p_m \leq 0.6 \text{ GeV}/c$ and $E_m \leq 100 \text{ MeV}$ in the perpendicular kinematics, the GA and GGA predictions differ only by less than $\simeq 3 - 4\%$.

*On leave from Bogoliubov Lab. Theor. Phys., 141980, JINR, Dubna, Russia

I. INTRODUCTION

One of the main aims of nowadays hadronic physics is the investigation of the limits of validity of the so called *Standard Model* of nuclei, i.e. the description of nuclei in terms of the solution of the non relativistic Schrödinger equation containing realistic nucleon-nucleon interactions. To this end, exclusive lepton scattering could be very useful for it might yield relevant information on the nuclear wave function, provided the initial and final states involved in the scattering process are described within a consistent, reliable approach. In the case of *few-body systems*, a consistent treatment of initial and final states is nowadays possible at low energies (see e.g. [1, 2] and References therein quoted), but at higher energies, when the number of partial waves sharply increases and nucleon-nucleon (NN) interaction becomes highly inelastic, the Schrödinger approach becomes impractical and other methods have to be employed. In the case of *complex nuclei*, additional difficulties arise even due to the approximations which are still necessary to solve the many-body problem. As a matter of fact, whereas fundamental progress has been made in recent years in the calculation of various properties of light nuclei (see e.g. [3] and [4] and References therein quoted), much remains to be done for the treatment of the continuum for which various approximate treatments of the final state cannot be avoided. In this context, it should be stressed that calculations involving few-body systems, where the ground state can be treated exactly, can also be very useful to investigate the limits of validity of various approximate schemes to treat the continuum and their possible extension to complex nuclei.

The aim of this paper is to present the results of a systematic theoretical investigation of the exclusive process $A(e, e'p)B$ off 2H and 3He , based on a reliable description of:

1. initial state correlations (ISC), treated by the use the status-of-the-art few-body wave functions [2] corresponding to the *AV18* interaction [5];
2. final state interactions (FSI), treated within a relativistic framework based upon the calculation of the relevant Feynman diagrams which describe the rescattering of the struck nucleon by the other $A - 1$ *spectator* nucleons of the target.

Whereas a correct treatment of ISC in few-body systems is automatically achieved by the use of realistic wave functions, the treatment of FSI is still matter of discussions. The approach we are going to use has several non trivial advantages, in that it allows one to work

within a relativistic framework provided by the use of Feynman diagrams and, moreover, it can be applied in principle to the treatment of exclusive $A(e, e'p)B$ processes off complex nuclei as well. It should be stressed, at this point, that the diagrammatic approach we are talking about is not a new one: it has been first formulated in Ref. [6] and [7] (see also Ref. [8]), within a spin-less treatment of particle-nucleus scattering, and applied subsequently to various types of high energy processes with nuclear targets. More recently, in Ref. [9], [10] and [11], the diagrammatic approach has been applied specifically to the treatment of the FSI in exclusive $A(e, e'p)B$ processes, and a Feynman diagram approach has also been used in Ref. [12], [13] and [14] to take into account off-shell effects both in inclusive, $A(e, e')X$, and exclusive, $A(e, e'p)B$, processes. The diagrammatic approach we are referring to, is a generalization of the standard Glauber approach (GA) [15] and could therefore be called Generalized Glauber approach (GGA) ([9], [10] and [11]). As it is well known, the application of the GA to the treatment of $A(e, e'p)B$ processes requires the following approximations: : i)the NN scattering amplitude is obtained within the eikonal approximation; ii) the nucleons of the spectator system $A - 1$ are stationary during the multiple scattering with the struck nucleon (the *frozen approximation*), and iii) only perpendicular momentum transfer components in the NN scattering amplitude are considered. In the GGA the *frozen approximation* is partly removed by taking into account the excitation energy of the $A - 1$ system, which results in a correction term to the standard profile function of GA, leading to an additional contribution to the longitudinal component of the missing momentum.

In the present paper we apply both the GA and the GGA to the calculation of the processes ${}^2H(e, e'p)n$, ${}^3He(e, e'p)D$, and ${}^3He(e, e'p)(np)$, and compare our results with available experimental data [16, 17, 18, 19, 20, 21]. The 3He wave function of the Pisa group [2], corresponding to the AV18 interaction [5], will be used in the calculations. We will consider kinematical conditions for which the effects from meson exchange currents (MEC) and delta excitation effects, are expected to be small corrections. Whenever possible, however, we will compare our results with the results by other authors which include these effects.

The structure of the paper is as follows: in Section II the basic formalism of lepton-hadron scattering is illustrated and the main formulae are obtained; in Section III the concept of Plane Wave Impulse Approximation (PWIA) and Spectral Function are reviewed; in Section IV, the GGA is introduced, the relevant Feynman diagrams which one needs to take into account the full FSI are analyzed, and the problem of the factorization of the lepton-nucleus

cross section within the GA and GGA is discussed; the results of the calculations and their comparison with available experimental data are presented in Section V, and the Conclusions are drawn in Section VI. Some details concerning the formal aspects of our approach are given in Appendices A and B.

Preliminary results of our calculations have been reported in Ref. [22] and [23].

II. BASIC FORMULAE OF LEPTON SCATTERING OFF NUCLEI

The one-photon-exchange diagram for the process $A(e, e'p)(A - 1)$, where $A - 1$ denotes a system of $A - 1$ nucleons in a bound or continuum state, is presented in Fig. 1 where the relevant four-momenta in the scattering processes are shown, namely the electron momenta before and after interaction are denoted by $k = (E, \mathbf{k})$, and $k' = (E', \mathbf{k}')$, respectively, the momentum of the target nucleus $P_A = (E_A, \mathbf{P}_A)$, and the momenta of the final proton and the final $A - 1$ system by $p_1 = (\sqrt{\mathbf{p}_1^2 + M_N^2}, \mathbf{p}_1)$ and $P_{A-1} = (\sqrt{\mathbf{P}_{A-1}^2 + (M_{A-1}^f)^2}, \mathbf{P}_{A-1})$ respectively, where M_N is the nucleon mass, $M_{A-1}^f = M_{A-1} + E_{A-1}^f$, and E_{A-1}^f is the *intrinsic* excitation energy of the $A - 1$ system.

Let us recall some useful formulae regarding the process described by the diagram shown in Fig. 1. The differential cross section for the exclusive process has the following form (see e.g. [24])

$$\frac{d^6\sigma}{dE'd\Omega' d^3\mathbf{p}_1} = \sigma_{Mott} \tilde{l}^{\mu\nu} W_{\mu\nu}^A \quad (1)$$

where $\sigma_{Mott} = \frac{4\alpha^2 E'^2 \cos^2 \frac{\theta}{2}}{Q^4}$ is the Mott cross section, α the fine-structure constant, $Q^2 = -q^2 = -(k - k')^2 = \mathbf{q}^2 - q_0^2 = 4EE' \sin^2 \theta/2$ the four-momentum transfer, $\theta \equiv \theta_{\mathbf{k}\mathbf{k}'}$ the scattering angle. The quantities $\tilde{l}_{\mu\nu}$ and $W_{\mu\nu}^A$ are the reduced leptonic and hadronic tensors, respectively; the former has the well known standard form ([24]), whereas the latter can be written as follows

$$W_{\mu\nu}^A = \frac{1}{4\pi M_A} \overline{\sum_{\alpha_A}} \sum_{\alpha_{A-1}, \alpha_N} (2\pi)^4 \delta^{(4)}(P_A + q - P_{A-1} - p_1) \times \\ \times \langle \alpha_A \mathbf{P} | \hat{J}_\mu^A(0) | \alpha_N \mathbf{p}_1, \alpha_{A-1} \mathbf{P}_{A-1} E_{A-1}^f \rangle \langle E_{A-1}^f \mathbf{P}_{A-1} \alpha_{A-1}, \mathbf{p}_1 \alpha_N | \hat{J}_\nu^A(0) | \alpha_A \mathbf{P}_A \rangle, \quad (2)$$

with α_i denoting the set of discrete quantum numbers of systems A , $A - 1$ and N . In Eq. 2 the vector $|\alpha_N \mathbf{p}_1, \alpha_{A-1} \mathbf{P}_{A-1} E_{A-1}^f\rangle$ consists asymptotically of a nucleus $A - 1$, with

momentum \mathbf{P}_{A-1} and intrinsic excitation energy E_{A-1}^f , and a nucleon with momentum \mathbf{p}_1 . It is well known that the general form of the hadronic tensor, restricted by the requirements of gauge-invariance, time-reversal invariance and parity conservation, depends upon four structure functions W_i^A , corresponding to the four independent scalars of the problem, viz.

$$W_{\mu\nu}^A = -W_1^A g_{\mu\nu} + W_2^A \frac{P_\mu^A P_\nu^A}{M_N^2} + W_3^A \frac{1}{(p_1 \cdot P^A)} \frac{1}{2} (P_\mu^A p_{1\nu} + P_\nu^A p_{1\mu}) + W_4^A \frac{p_{1\mu} p_{1\nu}}{M_N^2} \quad (3)$$

where the terms linear in q^μ do not appear thanks to the gauge invariance of the leptonic tensor. The structure of $W_{\mu\nu}^A$ can be obtained in a more physically transparent way by introducing, instead of W_i^A , another set of four scalar response functions. To this end, the complete set of polarization 4-vectors for a virtual photon

$$\epsilon_\pm^\mu = \mp \frac{1}{\sqrt{2}} (0, 1, \pm i, 0), \quad \epsilon_0^\mu = \frac{1}{\sqrt{Q^2}} (|\mathbf{q}|, 0, 0, q_0) \quad (4)$$

is introduced, with $\epsilon_\mu q^\mu = 0$, $\sum_\lambda \epsilon_\lambda^{*\mu} \epsilon_\lambda^\nu = -g^{\mu\nu} + \frac{q^\mu q^\nu}{q^2}$, and $\epsilon_\lambda^* = (-1)^\lambda \epsilon_{-\lambda}$ ($\lambda = \pm, 0$), to obtain

$$\tilde{l}^{\mu\nu} W_{\mu\nu}^A = \sum_{\lambda\lambda'} L_{\lambda\lambda'} W_{\lambda\lambda'}, \quad (5)$$

where

$$L_{\lambda\lambda'} = \epsilon_\lambda^\mu \tilde{l}_{\mu\nu} \epsilon_{\lambda'}^{*\nu}, \quad W_{\lambda\lambda'} = (-1)^{\lambda+\lambda'} \epsilon_\lambda^{*,\mu} W_{\mu\nu}^A \epsilon_{\lambda'}^\nu. \quad (6)$$

The four independent combinations of $\lambda\lambda'$ are usually chosen in the following form:

$$\begin{aligned} W_L^A &= \frac{|\mathbf{q}|^2}{Q^2} W_{00} ; & W_T^A &= W_{11} + W_{-1-1} ; \\ W_{LT}^A &= \frac{|\mathbf{q}|}{\sqrt{Q^2}} 2\text{Re} [W_{01} - W_{0-1}] ; & W_{TT}^A &= -2\text{Re} W_{1-1} ; \end{aligned} \quad (7)$$

defining, respectively, the longitudinal (L), transverse (T), longitudinal-transverse (LT) interference and transverse-transverse (TT) nuclear response functions. Two relevant experimentally measurable quantities which characterize the process are the *missing momentum* \mathbf{p}_m (i.e. the Center-of-Mass momentum of the $A-1$ system), and the *missing energy* E_m defined, respectively, by

$$\mathbf{p}_m = \mathbf{q} - \mathbf{p}_1 \quad E_m = \sqrt{P_{A-1}^2} + M_N - M_A = M_N + M_{A-1} - M_A + E_{A-1}^f = E_{min} + E_{A-1}^f \quad (8)$$

where $E_{min} = E_A - E_{A-1} = M_N + M_{A-1} - M_A$, and the (positive) ground-state energies of A and $A - 1$ are denoted by E_A and E_{A-1} , respectively. The exclusive cross section can then be written in the well-known form

$$\frac{d^6\sigma}{d\Omega'dE'd^3\mathbf{p}_m} = \sigma_{Mott} \sum_i V_i W_i^A(\nu, Q^2, \mathbf{p}_m, E_m) \quad (9)$$

where $i \equiv \{L, T, LT, TT\}$, and the kinematical factors V_i , in agreement with the definitions (7), have the following form:

$$\begin{aligned} V_L &= \frac{Q^4}{|\mathbf{q}|^4}, & V_T &= \tan^2(\theta/2) + \frac{Q^2}{2|\mathbf{q}|^2}, \\ V_{LT} &= \frac{Q^2}{\sqrt{2}|\mathbf{q}|^2} \sqrt{\tan^2(\theta/2) + \frac{Q^2}{|\mathbf{q}|^2}}, & V_{TT} &= \frac{Q^2}{2|\mathbf{q}|^2}. \end{aligned} \quad (10)$$

The evaluation of the nuclear response functions W_i^A requires the knowledge of the nuclear vectors $|\alpha_A \mathbf{P}_A\rangle$ and $|\alpha_N \mathbf{p}_1, \alpha_{A-1} \mathbf{P}_{A-1} E_{A-1}^f\rangle$ and the nuclear current operators $\hat{J}_\mu^A(0)$. Nowadays, there is no rigorous quantum field theory to describe, from first principles, a many body hadronic system, and one is forced to adhere to various approximations. Whereas at relatively low energies a consistent non relativistic treatment of the electro-disintegration of two- and three-body systems can be pursued, with increasing energy the treatment of the three- body final state requires proper approximations. In the present paper we describe the two- and three-body ground states in terms of realistic wave functions generated by modern two-body interactions [2], and treat the final state by a diagrammatic approach of the elastic rescattering of the struck nucleon with the nucleons of the $A - 1$ system. The relevant diagrams which, within such an approximation, replace the One-Photon-Exchange Feynman diagram of Fig. 1, are shown in Fig.2: the first one represents the *Plane Wave Impulse Approximation* (PWIA), whereas the other ones the final state rescattering (FSI).

Although the PWIA appears to have a limited range of validity, it is useful to analyze the results it predicts since, within such an approximation, the cross section is directly related to a quantity, the *Spectral Function*, which, in the case of few-body systems, can be calculated with high degrees of accuracy (see [25, 26, 27, 28]). The relevant point here is that, provided the FSI of the struck nucleon with the $A - 1$ system can be disregarded, the Spectral Function yields direct information on the nuclear wave function. For such a reason, we will present our results obtained within two distinct approaches:

1. the *PWIA* (Fig.2a), according to which the struck proton is described by a plane wave, whereas the $A - 1$ system in the final state, with momentum P_{A-1} , represents the bound or continuum state solutions of the Schrödinger equation with the same potential used to obtain the A-body wave function (note that some authors call PWIA the state in which *all* particles in the continuum are described by plane waves);
2. the *full FSI approach* (Fig. 2b,c), where the $A - 1$ system (in the ground or continuum states) is still described by the exact solution of the Schrödinger equation, and the interaction of the struck nucleon with the $A - 1$ nucleons is treated by evaluating the Feynman diagrams of Fig. 2, either in the GA or the GGA approximations.

III. THE PLANE WAVE IMPULSE APPROXIMATION AND THE NUCLEAR SPECTRAL FUNCTION

The main merit of the PWIA is that it allows one to express the *nuclear* response functions W_i^A in terms of the *nucleon* response functions which are very well known from $e - N$ experiments. The PWIA is based upon the following assumptions (for a detailed derivation of the PWIA see, e.g. Refs [29, 30])

1. The nuclear (\hat{J}_ν^A) current operator is the sum of one-body nucleon (\hat{J}_ν^N) current operators, *viz*

$$\hat{J}_\nu^A(Q^2) = \sum_{N=1}^A \hat{J}_\nu^N(Q^2), \quad (11)$$

i.e. the sum of currents for Dirac particles treated within an effective quantum field theory, i.e. with their internal structure described by some phenomenological form factors; therefore the effective current operators for nucleons are Q^2 -dependent and so is the nuclear current operator, where the Q^2 -dependence of \hat{J}_ν^A and \hat{J}_ν^N in Eq. (11) can in principle differ;

2. the final hadronic state $|\alpha_N \mathbf{p}_1, \alpha_{A-1} \mathbf{P}_{A-1} E_{A-1}^f\rangle$ asymptotically consists of two non interacting (i.e. plane wave states) systems, i.e.

$$|\alpha_N \mathbf{p}_1, \alpha_{A-1} \mathbf{P}_{A-1} E_{A-1}^f\rangle = \hat{\mathcal{A}}\{|\alpha_N \mathbf{p}_1\rangle |\alpha_{A-1} \mathbf{P}_{A-1} E_{A-1}^f\rangle\}, \quad (12)$$

where $\hat{\mathcal{A}}$ is a proper anti-symmetrization operator;

3. the incoherent contributions leading to the emission of nucleon N , due to the interaction of γ^* with $A - 1$, are disregarded, which is always well justified at high momentum transfers.

It is straightforward to show that if one: i) adheres to the above assumptions, ii) inserts in (2) a complete set of plane waves and $A - 1$ states, iii) imposes conservation of linear momentum, then, by comparing the hadronic tensor for the nucleus A , with the hadronic tensor for the nucleon N ,

$$W_{\mu\nu}^N = \frac{1}{4\pi M_N} \overline{\sum_{\alpha_N}} \sum_{\alpha'_N} (2\pi)^4 \delta^{(4)}(p + q - p_1) \times \\ \times \langle \alpha_N \mathbf{p}_1 | \hat{J}_\mu^N(0) | \alpha'_N \mathbf{p}'_1 \rangle \langle \alpha'_N \mathbf{p}'_1 | \hat{J}_\nu^N(0) | \alpha_N \mathbf{p}_1 \rangle \quad (13)$$

one obtains the following expression for the cross section of the process $A(e, e'p)(A - 1)$ [31]

$$\frac{d^6\sigma}{dE' d\Omega' d\mathbf{p}_m} = K(\bar{Q}^2, x, \mathbf{p}_m) \sigma^{eN}(\bar{Q}^2, \mathbf{p}_m) P_A(|\mathbf{k}_1|, E) \quad (14)$$

where $\bar{Q}^2 = \mathbf{q}^2 - \bar{q}_0^2$ ($\bar{q}_0 = q_0 + M_A - \sqrt{(\mathbf{k}_1^2 + (M_{A-1}^f)^2) - \sqrt{\mathbf{k}_1^2 + M_N^2}}$), $K(\bar{Q}^2, x, \mathbf{p})$ is a kinematical factor, $\sigma^{eN}(\bar{Q}^2, \mathbf{p}_m)$ the cross section describing electron scattering by an off-shell nucleon, $x = Q^2/2M_N q_0$ the Bjorken scaling variable, $\mathbf{k}_1 = -\mathbf{p}_m$ the nucleon momentum before interaction, $E = E_{mis} = E_{min} + E_{A-1}^f$ the *removal energy* and, eventually, $P(|\mathbf{k}_1|, E)$ the nucleon Spectral Function

$$P(|\mathbf{k}_1|, E) = \frac{1}{(2\pi)^3} \frac{1}{2J_A + 1} \sum_f \sum_{\mathcal{M}_A, \mathcal{M}_{A-1}, \sigma_N} \left| \langle \alpha_A \mathbf{P} | \alpha_N \mathbf{k}_1, \alpha_{A-1} \mathbf{P}_{A-1} E_{A-1}^f \rangle \right|^2 \times \quad (15) \\ \times \delta(E - (E_{A-1}^f + E_{min}))$$

with the sum over f including all possible discrete and continuum states of the $A - 1$ system.

The Spectral Function for the Deuteron (D) has a particularly simple form, viz.

$$P_D(|\mathbf{k}_1|, E) = n_D(|\mathbf{k}_1|) \delta(E - \epsilon_D) \quad (16)$$

where ϵ_D is the (positive) binding energy of the deuteron and

$$n_D(|\mathbf{k}_1|) = \frac{1}{2\pi^2} \left(u_S^2(|\mathbf{k}_1|) + u_D^2(|\mathbf{k}_1|) \right) \quad (17)$$

the nucleon momentum distribution normalized as follows

$$\int n_D(|\mathbf{k}_1|)d^3\mathbf{k}_1 = \frac{2}{\pi} \int |\mathbf{k}_1|^2 d|\mathbf{k}_1| (u_S^2(|\mathbf{k}_1|) + u_D^2(|\mathbf{k}_1|)) = 1 \quad (18)$$

where u_S and u_D are the $L = 0$ and $L = 2$ radial components defining the deuteron wave function

$$\Psi_D^{\mathcal{M}_2}(\mathbf{k}_1) \equiv 4\pi \sum_{L,M_L,S_{12}} \langle LM_L 1S_{12} | 1\mathcal{M}_2 \rangle u_L(|\mathbf{k}_1|) Y_{LM_L}(\mathbf{n}) \chi_{1S_{12}}, \quad (19)$$

with \mathcal{M}_2 denoting the projection of the deuteron spin, and

$$\chi_{1S_{12}} = \sum_{\nu_1, \nu_2} \left\langle \frac{1}{2} \nu_1 \frac{1}{2} \nu_2 | 1S_{12} \right\rangle \chi_{\frac{1}{2} \nu_1} \chi_{\frac{1}{2} \nu_2} \quad (20)$$

In the case of $A=3$, the proton Spectral Function consists of two parts,

$$P_{He}(|\mathbf{k}_1|, E) = P_{gr}(|\mathbf{k}_1|, E) + P_{ex}(|\mathbf{k}_1|, E), \quad (21)$$

The first one, or *ground*, part has the following form

$$P_{gr}(|\mathbf{k}_1|, E) = n_{gr}(|\mathbf{k}_1|) \delta(E - E_{min}) \quad (22)$$

where $E_{min} = |E_3| - |E_2| \approx 5.49 MeV$, and $n_{gr}(|\mathbf{k}_1|)$, which corresponds to the two-body break-up (2bbu) channel ${}^3He \rightarrow D + p$, is (hereafter, the projection of the spin of nucleon i will be denoted by s_i)

$$n_{gr}(|\mathbf{k}_1|) = \frac{1}{(2\pi)^3} \frac{1}{2} \sum_{\mathcal{M}_3, \mathcal{M}_2, s_1} \left| \int e^{-i\rho\mathbf{k}_1} \chi_{\frac{1}{2} s_1}^\dagger \Psi_D^{\mathcal{M}_2\dagger}(\mathbf{r}) \Psi_{He}^{\mathcal{M}_3}(\boldsymbol{\rho}, \mathbf{r}) d\boldsymbol{\rho} d\mathbf{r} \right|^2 \quad (23)$$

In Eq.(23) $\Psi_{He}^{\mathcal{M}_3}(\boldsymbol{\rho}, \mathbf{r})$ is the 3He wave function, \mathcal{M}_3 the projection of the spin of 3He , and \mathbf{r} and $\boldsymbol{\rho}$ the Jacobi coordinates describing, respectively, the motion of the spectator pair and the motion of the struck (active) nucleon with respect to the CM of the pair.

The second, or *excited*, part P_{ex} of $P_{He}(|\mathbf{k}_1|, E)$, corresponds to the three-body break-up (3bbu) channel ${}^3He \rightarrow (np) + p$ and can be written as follows

$$\begin{aligned} P_{ex}(|\mathbf{k}_1|, E) &= \frac{1}{(2\pi)^3} \frac{1}{2} \sum_{\mathcal{M}_3, S_{23}, s_1} \int \frac{d^3\mathbf{t}}{(2\pi)^3} \left| \int e^{-i\rho\mathbf{k}_1} \chi_{\frac{1}{2} s_1}^\dagger \Psi_{np}^{\mathbf{t}\dagger}(\mathbf{r}) \Psi_{He}^{\mathcal{M}_3}(\boldsymbol{\rho}, \mathbf{r}) d\boldsymbol{\rho} d\mathbf{r} \right|^2 \times \\ &\times \delta \left(E - \frac{\mathbf{t}^2}{M_N} - E_3 \right), \end{aligned} \quad (24)$$

where $\Psi_{np}^{\mathbf{t}}(\mathbf{r})$ is the two-body continuum wave functions characterized by spin projection S_{23} and by the relative momentum $\mathbf{t} = \frac{\mathbf{k}_2 - \mathbf{k}_3}{2}$ of the np pair in the continuum. Obviously, for the neutron Spectral Function, only the excited part (24) contributes.

In Fig. 3 we show the Spectral Function of 3He obtained using the variational three-body wave function by the Pisa group [2] within a correlated variational approach using the realistic AV18 potential [5] (see Appendix A). The two-body wave function entering Eq. (24) has been obtained by solving the Schrödinger equation for the continuum using the same AV18 two nucleon potential. Our results for the Spectral Function agree with the ones obtained in Ref. [27], where the same three-body wave function has been used. The normalization of the Proton Spectral Function has been fixed to 2 (two protons) and the normalization of the neutron Spectral Function to one. In Fig. 3 we also show the results predicted by the *Plane Wave Approximation* (PWA), which corresponds to the replacement of the continuum interacting $(n-p)$ pair wave function with two plane waves. The left panel of Fig. 3 shows n_{gr} and the right panel P_{ex} . It can be seen that: i) P_{ex} exhibits maxima centered approximately at $E_m \sim \frac{\mathbf{k}_1^2}{4M_N}$, ii) around these values of E_m and \mathbf{k}_1 the Spectral Functions, calculated disregarding the interaction in the NN -pair in the continuum (the *Plane Wave Approximation*) and taking it into account (PWIA), are almost identical, in agreement with the results obtained long ago [28] with the Spectral Function corresponding to the Reid Soft Core Interaction [32]. The region centered at $E_m \sim \frac{\mathbf{k}_1^2}{4M_N}$ is the so-called two-nucleon correlation region, when one of the nucleons of the NN -pair is fast, the other one being basically at rest [33] (for an improved description see [34]). Then the fast nucleon becomes strongly correlated with the active nucleon (the proton, in the case of the proton Spectral Function, or the neutron, in the case of the neutron Spectral Function) forming a correlated pair which carries most of the nuclear momentum. In this case, it is intuitively expected that the slow nucleon acts as a passive spectator and, consequently, only the interaction in the correlated pair can be relevant for the Spectral Function. Hence, in this region the calculations including or omitting the interaction in the spectator pair are expected to provide essentially the same results, as confirmed by present and previous calculations of the Spectral Function [22], [23], [28]. The situation which has been just described, is clearly illustrated in Fig. 4, where the 3-dimensional neutron Spectral Function is presented.

The PWIA results suggest that experimental insight about the structure of the nuclear wave function at short distances can be obtained from $A(e, e'p)(A - 1)$ processes, provided the PWIA entirely exhausts the reaction mechanism. Unfortunately, we know that in many cases the simplified PWIA mechanism fails to describe the experimental data (see, e.g. a recent discussions in ref. [35]). However, a properly chosen kinematics can still leave room for studying NN correlations. It is clear, from Figs. 3 and 4, that such a kinematics should be located around the two-nucleon correlation region in order to exclude, at least the influence of the final state interaction between the spectator nucleons. This requires high values of the missing energy and momentum of the active nucleon (see Fig. 4). Another important condition is that the range of $|\mathbf{q}|$ and q_0 should not be too far from the quasi-elastic peak, where $x \simeq 1$. In this case the corrections from the off mass shell effects and meson production are minimized and only the final state interaction of the hit nucleon with the spectators becomes relevant. However, it should always be kept in mind, that if a region exists where the interaction *in* the spectator pair (the $A - 1$ system in case of complex nuclei) can be neglected, this is no guarantee that the interaction of the struck nucleon *with* the nucleons of the spectator pairs (the $A - 1$ system), can be neglected as well. Moreover, experimental data might be available in regions where the full interaction in the final state may be relevant. It is clear therefore that one has to go beyond the PWIA, which is precisely the aim of the present paper. The effects of the full FSI on the process ${}^3He(e, e'2p)n$ have been recently investigated, treating the FSI within the GA [36]. In the present paper we will investigate the same topic in $A(e, e'p)X$ process off 2H and 3He within both the GA and the GGA approximations.

IV. THE FULL FINAL STATE INTERACTION WITHIN THE GENERALIZED EIKONAL APPROXIMATION

Let us consider the interaction of the incoming virtual photon, γ^* , with a bound nucleon (the active nucleon) of low virtuality ($p^2 \sim M_N^2$) at a kinematics not very different from the quasi-elastic one, i.e. corresponding to $x \sim 1$. In the quasi-elastic kinematics, the virtuality of the struck nucleon after γ^* -absorbtion is also rather low and, provided \mathbf{p}_1 is sufficiently high, nucleon rescattering with the "spectator" $A - 1$ can be described to a large extent in terms of multiple elastic scattering processes in the forward direction (in the

system of reference where the target nucleon is at rest). These rescattering processes are diagrammatically depicted in Fig. 2 where, as in the rest of this paper, the internal and intermediate state momenta are denoted by k_i 's and the final state momenta by p_i 's. The diagrams essentially describe the process of multiple scattering in the most general case, in the assumption that all intermediate nucleons are on-shell. The low virtuality (before and after γ^* absorption) of the active nucleon, coupled with the forward propagation, allows one to simplify the description of the final state interaction, which can be treated within the eikonal approximation. Before illustrating in detail the approach we have used to treat FSI in $(e, e'p)$ reactions, we would like to discuss an important related issue (see also [37]), namely the validity of the factorization approximation, frequently used in calculations at high Q^2 , and consisting in factorizing the $(e, e'p)$ cross section into an e.m. and a nuclear parts, in spite of the fact that factorization, holding exactly in PWIA, is violated when FSI is taken into account. In the next Section the factorization approximation will be discussed within the GA and the GGA.

A. The FSI in $(e, e'p)$ processes and the factorization of the cross section

Most of the problems have to be faced when trying to develop a fully covariant treatment of FSI, arise because of the hadron's spins. Therefore, let us rewrite the hadronic tensor (Eq. (2)) in the following, fully equivalent form, which however exhibits explicitly the dependence upon the spin quantum numbers

$$W_{\mu\nu}^A = \frac{1}{4\pi M_N} \overline{\sum_{\alpha_A} \sum_{\alpha_{A-1}, s_1} T_\mu^\dagger(\mathcal{M}_A, \mathcal{M}_{A-1}, s_1) T_\nu(\mathcal{M}_A, \mathcal{M}_{A-1}, s_1)} \times (2\pi)^4 \delta^{(4)}(P_A + q - P_{A-1} - p_1) \quad (25)$$

where T_μ is a short-hand notation for the transition matrix element

$$T_\mu(\mathcal{M}_A, \mathcal{M}_{A-1}, s_1) \equiv \langle \alpha_{A-1} \mathbf{P}_{A-1} E_{A-1}^f, s_1 \mathbf{p}_1 | \hat{J}_\mu^A(0) | \alpha_A \mathbf{P}_A \rangle \quad (26)$$

The basic assumption underlying the eikonal diagrammatic treatment of FSI at high Q^2 is that the transition matrix element T_μ for a nucleus A can be written in the following form

$$T_\mu(\mathcal{M}_A, \mathcal{M}_{A-1}, s_1) = \sum_{n=0}^{A-1} T_\mu^{(n)}(\mathcal{M}_A, \mathcal{M}_{A-1}, s_1) \quad (27)$$

where the superscript (n) corresponds to the order of rescattering of the struck particle with the $A - 1$ nucleons (the "spectators" nucleons), namely $T_\mu^{(0)}$ corresponds to the PWIA (no rescattering), $T_\mu^{(1)}$ to the single rescattering of the struck nucleons with the spectators ones, $T_\mu^{(2)}$ to double rescattering, and so on. Such an approach is expected to be valid either at high energies when particles propagate mostly in the forward direction along the direction of the three-momentum transfer \mathbf{q} , or when the momentum of the struck nucleon \mathbf{p}_1 relative to $A - 1$ is sufficiently high; in both cases the eikonal approximation could be applied. The calculation of the rescattering part of T_μ in terms of Feynman diagrams appears in principle to be a prohibitive relativistic task due, as previously stressed, to the treatment of the spin. A relevant simplification occurs if the cross section factorizes into the e.m. and the nuclear parts and, as a matter of fact, many calculations performed within the eikonal approximation treatment of the FSI, simply assumes factorization. Let us try to analyze the limits of validity of such an assumption, and to this end let us consider the deuteron. In this case the Feynman diagrams describing rescattering are given in Fig.5, and the corresponding matrix element is

$$T_\mu(\mathcal{M}_2, s_1, s_2) = T_\mu^{(0)}(\mathcal{M}_2, s_1, s_2) + T_\mu^{(1)}(\mathcal{M}_2, s_1, s_2) \quad (28)$$

where \mathcal{M}_2 , s_1 and s_2 are the spin projection of the deuteron, and of nucleon "1" (the active nucleon) and nucleon "2" (the spectator nucleon) in the final state. Eq. (28) obviously states that in the deuteron the interaction between the struck and the spectator nucleon can occur only via single rescattering. The cross section of the process is given by

$$\frac{d^6\sigma}{dE'd\Omega'} = \sigma_{Mott} \tilde{l}^{\mu\nu} L_{\mu\nu}^D \frac{d^3p_1}{(2\pi)^3 2E_1} \frac{d^3p_2}{(2\pi)^3 2E_2} \quad (29)$$

where $E_i = \sqrt{\mathbf{p}_i^2 + M^2}$, and the hadronic tensor is as follows

$$L_{\mu\nu}^D = \frac{1}{2M_D} \frac{1}{3} \sum_{\mathcal{M}_2, s_1, s_2} T_\mu^\dagger(\mathcal{M}_2, s_1, s_2) T_\nu(\mathcal{M}_2, s_1, s_2) (2\pi)^4 \delta^{(4)}(P_D + q - p_1 - p_2) \quad (30)$$

Let us now obtain the factorization of the cross section, expressed in terms of the hadronic tensor (30), within a fully covariant approach.

1. The PWIA and the factorization of the cross section.

The PWIA for the process ${}^2H(e, e'p)n$ within a covariant Feynman diagram approach has been considered by various authors (see e.g. [38, 39, 40]). The matrix element $T_\mu = T_\mu^{(0)}$, in such a case, has the following form

$$\begin{aligned} T_\mu^{(0)}(\mathcal{M}_2, s_1, s_2) &= \\ &= \frac{1}{2M_N} \sum_{\tilde{s}_1} J_\mu^{eN}(Q^2, p_1, k_1, \tilde{s}_1, s_1) [\bar{u}(\mathbf{k}_1, \tilde{s}_1) \Phi_D^{\mathcal{M}_2}(k_1, k_2)(\hat{k}_2 + M_N)v(\mathbf{k}_2, s_2)] \end{aligned} \quad (31)$$

where

$$J_\mu^{eN}(Q^2, p_1, k_1, \tilde{s}_1, s_1) = \langle \mathbf{p}_1, s_1 | \Gamma_\mu^{\gamma^*N}(Q^2, k_1^2) | \mathbf{k}_1, \tilde{s}_1 \rangle, \quad (32)$$

$\Gamma_\mu^{\gamma^*N}(Q^2, k_1^2)$ is the e.m. vertex, and $\Phi_D^{\mathcal{M}_2}(k_1, k_2)$ the covariant deuteron amplitude corresponding to the $D \rightarrow (pn)$ vertex. The explicit form of the amplitude $\Phi_D^{\mathcal{M}_2}(k_1, k_2)$ depends upon the specific covariant model used to describe the deuteron and could be found elsewhere (see e.g., [38, 39, 41]); here, without loss of generality, we will use the Bethe-Salpeter (BS) formalism according to Refs. [41] and [40].

When Eq. (31) is placed in Eq. (30), the e.m. and nuclear parts gets coupled by the summation over the intermediate spins \tilde{s}_1 and \tilde{s}_1' . However, it can be shown (see Appendix B) that the square of the expression in brackets in Eq.(31) after summation over \mathcal{M}_2 and s_2 yields a δ function $\delta_{\tilde{s}_1 \tilde{s}_1'}$, i.e. becomes diagonal in \tilde{s}_1 ; this leads to the decoupling between the e.m and the nuclear parts in Eq.(31), with the resulting hadronic tensor given by

$$\begin{aligned} L_{\mu\nu}^D &= \frac{1}{2M_D} \frac{1}{3} \sum_{\mathcal{M}_2, s_1, s_2} T_\mu^\dagger(M, s_1, s_2) T_\nu(M, s_1, s_2) = \\ &= 2M_D \left(2E_{\mathbf{p}_1} 2E_{\mathbf{k}_1} L_{\mu\nu}^{eN}(Q^2, p_1, k_1) \right) n_D(|\mathbf{k}_1|) (2\pi)^4 \delta^{(4)}(P_D + q - p_1 - p_2) .. \end{aligned} \quad (33)$$

In Eq. (33), n_D is the deuteron momentum distribution given by (cf. Eq. (17))

$$\begin{aligned} n_D(|\mathbf{k}_1|) &= \frac{1}{3} \sum_{\mathcal{M}_2, \tilde{s}_1, s_2} \left| [\bar{u}(\mathbf{k}_1, \tilde{s}_1) \Phi_D^{\mathcal{M}_2}(k_1, k_2)(\hat{k}_2 + M_N)v(\mathbf{k}_2, s_2)] \right|^2 = \\ &= \frac{1}{3} \sum_{\mathcal{M}_2, \tilde{s}_1, s_2} \left| \langle \tilde{s}_1, s_2 | \Psi_D^{\mathcal{M}_2}(\mathbf{k}_1) \rangle \right|^2 = \frac{1}{2\pi^2} (u_S^2(|\mathbf{k}_1|) + u_D^2(|\mathbf{k}_1|)) \end{aligned} \quad (34)$$

where the (covariant) deuteron wave function has been cast in a form similar to the non relativistic one (cf. Eqs. (19) and (20)) with the scalar parts of the wave function, $u_L(|\mathbf{k}|)$'s, related to the corresponding vertex functions, $G_L(k_1^2, k_2^2 = M_N^2)$, by a well known definition (see Eqs. (B14) and (B15)) leading to

$$u_L(|\mathbf{k}|) \sim \sqrt{2M_N} \frac{G_L(|\mathbf{k}|, k_{10} = M_D - E_{\mathbf{k}})}{k^2 - M_N^2} \quad (35)$$

Placing Eq. (33) in Eq. (29) the well known factorized form for the cross section is obtained, *viz.*

$$\frac{d^6\sigma}{dE'd\Omega'd\mathbf{p}_m} = K(\bar{Q}^2, x, \mathbf{p}_m) \sigma^{eN}(\bar{Q}^2, \mathbf{p}_m) n_D(|\mathbf{k}_1|) \delta(q_0 + M_D - E_{\mathbf{k}_1 + \mathbf{q}} - E_{\mathbf{k}_1}) \quad (36)$$

We reiterate that factorization has been obtained because the sum over s_2 and \mathcal{M}_2 in (30) leads to the appearance of a delta function $\delta_{\tilde{s}'_1, \tilde{s}_1}$, which means, in turn, that the square of $T_\mu^{(0)}$ becomes diagonal in \tilde{s}_1 . This particular (exact) result is part of a more general assertion that within the PWIA the nuclear Spectral Function is always diagonal in spins [31]. Let us now consider FSI; in this case the tensor (30) is off-diagonal in spins and factorization does not occur. However, we will show in the following Section that under certain kinematical conditions, satisfied to a large extent by the GA and GGA, factorization can be recovered.

2. FSI: the single scattering contribution and factorization of the cross section.

Let us compute the second diagram of Fig. 5. To this end, we introduce a two-nucleon scattering operator \hat{T} in terms of which the elastic scattering amplitude f^{NN} , describing the elastic scattering of two on-shell nucleons, could be defined, namely

$$f_{\tilde{s}_1 \tilde{s}_2; s_1, s_2}^{NN}(\mathbf{p}_1, \mathbf{p}_2; \mathbf{k}_1, \mathbf{k}_2) = \bar{u}(\mathbf{p}_1, s_1) \bar{u}(\mathbf{p}_2, s_2) \hat{T} u(\mathbf{k}_1, \tilde{s}_1) u(\mathbf{k}_2, \tilde{s}_2), \quad (37)$$

which is obviously the free NN scattering amplitude; for a bound nucleon one has in principle to consider off-shell effects but in the GGA no virtuality is considered; this could be done for example by the approach of Ref. [13], by introducing cut-off form factors in the corresponding nucleon lines, which formally leads to two Feynman diagrams with different "nucleonic" masses. In presence of FSI, the transition matrix element is

$$T_\mu(\mathcal{M}_2, s_1, s_2) = T_\mu^{(0)}(\mathcal{M}_2, s_1, s_2) + T_\mu^{(1)}(\mathcal{M}_2, s_1, s_2) \quad (38)$$

with $T_\mu^{(0)}$ given again by Eq. (31) and $T_\mu^{(1)}$ given by the following form (note that henceforth we always mean $\mathbf{k}_1 = -\mathbf{k}_2$)

$$\begin{aligned} T_\mu^{(1)}(\mathcal{M}_2, s_1, s_2) &= \frac{1}{2M_N} \sum_{\tilde{s}_1 \tilde{s}_1' \tilde{s}_2} \int \frac{d^4 k_2}{i(2\pi)^4} \frac{f_{\tilde{s}_1' \tilde{s}_2; s_1, s_2}^{NN}(\mathbf{p}_1, \mathbf{p}_2, \mathbf{k}_1', \mathbf{k}_2)}{k_1'^2 - M_N^2 + i\varepsilon} \times \\ &\times \left[\bar{u}(\mathbf{k}_1', \tilde{s}_1') \Gamma_\mu^{\gamma^* N}(Q^2, k_1'^2) u(\mathbf{k}_1, \tilde{s}_1) \right] \left[\bar{u}(\mathbf{k}_1, \tilde{s}_1) \Phi_D^{\mathcal{M}_2}(k_1, k_2) v(\mathbf{k}_2, \tilde{s}_2) \right] \end{aligned} \quad (39)$$

The full matrix element will therefore be

$$\begin{aligned} T_\mu(\mathcal{M}_2, s_1, s_2) &= \\ &= \frac{1}{2M_N} \sum_{\tilde{s}_1} J_\mu^{eN}(Q^2, \mathbf{p}_1, \mathbf{p}_m, \tilde{s}_1, s_1) \left[\bar{u}(\mathbf{k}_1, \tilde{s}_1) \Phi_D^{\mathcal{M}_2}(k_1, k_2) (\hat{k}_2 + M_N) v(\mathbf{k}_2, s_2) \right] + \\ &+ \frac{1}{2M_N} \sum_{\tilde{s}_1 \tilde{s}_1' \tilde{s}_2} \int \frac{d^4 k_2}{i(2\pi)^4} \frac{f_{\tilde{s}_1' \tilde{s}_2; s_1, s_2}^{NN}(\mathbf{p}_1, \mathbf{p}_2, \mathbf{k}_1', \mathbf{k}_2)}{k_1'^2 - M_N^2 + i\varepsilon} \times \\ &\times \left[\bar{u}(\mathbf{k}_1', \tilde{s}_1') \Gamma_\mu^{\gamma^* N}(Q^2, k_1'^2) u(\mathbf{k}_1, \tilde{s}_1) \right] \left[\bar{u}(\mathbf{k}_1, \tilde{s}_1) \Phi_D^{\mathcal{M}_2}(k_1, k_2) v(\mathbf{k}_2, \tilde{s}_2) \right] \end{aligned} \quad (40)$$

When Eq. (40) is placed into Eq. (30), the resulting equation is not diagonal in the spin quantum numbers and factorization does not hold. Let us however consider the basic assumptions underlying the eikonal multiple scattering approach, viz.:

1. the momentum transfer $\boldsymbol{\kappa}$ in the elastic rescattering is small and mostly transverse i.e.

$$\boldsymbol{\kappa} = \mathbf{p}_1 - \mathbf{k}_1' = \mathbf{k}_2 - \mathbf{p}_2 \simeq \mathbf{k}_{2\perp} - \mathbf{p}_{2\perp} = \boldsymbol{\kappa}_\perp \quad (41)$$

2. the spin-flip part of the NN amplitude is very small, which means that, taking into account Point 1, one can write

$$f_{\tilde{s}_1' \tilde{s}_2; s_1, s_2}^{NN}(\mathbf{p}_1, \mathbf{p}_2, \mathbf{k}_1', \mathbf{k}_2) \approx \delta_{\tilde{s}_1', s_1} \delta_{\tilde{s}_2, s_2} f^{NN}(\boldsymbol{\kappa}_\perp) \quad (42)$$

which is realized either at high values of the 3-momentum transfers \mathbf{q} , or at high values of the momentum \mathbf{p}_1 of the struck nucleon relative to the $A - 1$ spectator nucleons.

If the above conditions are satisfied, Eq. (39) assumes the following form (cf. Appendix B)

$$T_\mu^{(1)}(\mathcal{M}_2, s_1, s_2) \simeq \sum_{\tilde{s}_1} J_\nu^{eN}(Q^2, \mathbf{p}_m, \mathbf{p}_1, \tilde{s}_1, s_1) \frac{1}{2M_N} \int \frac{d^4 k_2}{i(2\pi)^4} \frac{f^{NN}(\boldsymbol{\kappa}_\perp)}{k_1'^2 - M_N^2 + i\varepsilon} \times \\ \times \left[\bar{u}(\mathbf{k}_1, \tilde{s}_1) \Phi_D^{\mathcal{M}_2}(k_1, k_2) v(\mathbf{k}_2, s_2) \right] \quad (43)$$

and one can write

$$T_\mu(\mathcal{M}_2, s_1, s_2) \simeq \\ \simeq \frac{1}{2M_N} \sum_{\tilde{s}_1} J_\nu^{eN}(Q^2, \mathbf{p}_m, \mathbf{p}_1, \tilde{s}_1, s_1) \times \\ \times \left\{ \left[\bar{u}(\mathbf{k}_1, \tilde{s}_1) \Phi_D^{\mathcal{M}_2}(k_1, k_2) (\hat{k}_2 + M_N) v(\mathbf{k}_2, s_2) \right] + \right. \\ \left. + \int \frac{d^4 k_2}{i(2\pi)^4} \frac{f^{NN}(\boldsymbol{\kappa}_\perp)}{k_1'^2 - M_N^2 + i\varepsilon} \left[\bar{u}(\mathbf{k}_1, \tilde{s}_1) \Phi_D^{\mathcal{M}_2}(k_1, k_2) v(\mathbf{k}_2, s_2) \right] \right\} \quad (44)$$

It can be seen that $T_\mu^{(0)}$ and $T_\mu^{(1)}$ in Eq. (44) have very similar structures, except that in $T_\mu^{(1)}$ the vector \mathbf{k}_2 is now an integration variable, since $\mathbf{k}_2 \neq \mathbf{p}_2$. When Eq. (30) is evaluated, with T_μ given by Eq. (44) and assuming soft NN rescattering (low values of $\boldsymbol{\kappa}_\perp$), the main contribution in the integral over \mathbf{k}_2 results from the region where $\mathbf{k}_2 \sim \mathbf{p}_2$ and this, in turn, originates again a delta function $\delta_{\tilde{s}_1 s_1}$ (See Appendix B) and the hadronic tensor becomes

$$L_{\mu\nu}^D = \frac{1}{2M_D} \frac{1}{3} \sum_{\mathcal{M}_2, s_1, s_2} T_\mu^\dagger(\mathcal{M}_2, s_1, s_2) \cdot T_\nu(\mathcal{M}_2, s_1, s_2) (2\pi)^4 \delta^{(4)}(P_D + q - p_1 - p_2) \simeq \\ \simeq \frac{1}{2} \sum_{\tilde{s}_2, s_1} \left[J_\mu^{eN\dagger}(Q^2, \mathbf{p}_m, \mathbf{p}_1, \tilde{s}_2, s_1) \cdot J_\nu^{eN}(Q^2, \mathbf{p}_m, \mathbf{p}_1, \tilde{s}_2, s_1) \right] \times \\ \times \frac{1}{(2M_N)^2} \sum_{\mathcal{M}_2 \tilde{s}_1, s_2} \left| \left[\bar{u}(\mathbf{k}_2, \tilde{s}_1) \Phi_D^{\mathcal{M}_2}(k_1, k_2) (\hat{k}_2 + M_N) v(\mathbf{k}_2, s_2) \right]_{k_2=p_2} + \right. \\ \left. + \int \frac{d^4 k_2}{i(2\pi)^4} \frac{f^{NN}(\boldsymbol{\kappa}_\perp)}{k_1'^2 - M_N^2 + i\varepsilon} [\bar{u}(\mathbf{k}_2, \tilde{s}_1) \Phi_D^{\mathcal{M}_2}(k_1, k_2) v(\mathbf{k}_2, s_2)] \right|^2 \times \\ \times (2\pi)^4 \delta^{(4)}(P_D + q - p_1 - p_2) \quad (45)$$

and the factorization of the e.m. and the nuclear parts is recovered. Eq. (45) could be written in a more familiar form if one integrates over k_{20} by taking into account the pole in the amplitude $\Phi_D^{\mathcal{M}_2}(k_1, k_2)$ ($k_{20} = E_{\mathbf{k}}$) and neglecting the pole from the active propagator,

which is located at large values of k_{20} and does not contribute to the integral. Using (34)-(35) one obtains ($\int d^4k/[i(2\pi)^4] \rightarrow \int d^3k/[(2E_{\mathbf{k}}(2\pi)^3)]$)

$$\begin{aligned} L_{\mu\nu}^D &\simeq 2M_D \left[2E_{\mathbf{p}_1} 2E_{\mathbf{p}_m} L_{\mu\nu}^N(Q^2, \mathbf{p}_m, \mathbf{p}_1) \right] \times \\ &\times \sum_{\mathcal{M}_2, s_1, s_2} \left| \left\langle s_1, s_2 | \Psi_D^{\mathcal{M}_2}(\mathbf{k}_2) \right\rangle \right|_{k_2=p_2} + \int \frac{d^3k_2}{2E_{\mathbf{k}_2}(2\pi)^3} \frac{f^{NN}(\boldsymbol{\kappa}_\perp)}{k_1'^2 - M_N^2 + i\varepsilon} \left\langle s_1, s_2 | \Psi_D^{\mathcal{M}_2}(\mathbf{k}_2) \right\rangle \right|^2 \times \\ &\times (2\pi)^4 \delta^{(4)}(P_D + q - p_1 - p_2) \end{aligned} \quad (46)$$

By placing the above equation in Eq. (29), one obtains

$$\frac{d^6\sigma}{dE'd\Omega'd\mathbf{p}_m} = K(\bar{Q}^2, x, \mathbf{p}_m) \sigma^{eN}(\bar{Q}^2, \mathbf{p}_m) n_D^{FSI}(\mathbf{p}_m) \delta(q_0 + M_D - E_{\mathbf{p}_1+\mathbf{q}} - E_{\mathbf{p}_2}) \quad (47)$$

where the *Distorted Momentum Distribution* n_D^{FSI} are

$$\begin{aligned} n_D^{FSI}(\mathbf{p}_m) &= \\ &= \sum_{\mathcal{M}_2, s_1, s_2} \left| \left\langle s_1, s_2 | \Psi_D^{\mathcal{M}_2}(\mathbf{k}_2) \right\rangle \right|_{k_2=p_2} + \int \frac{d^3k_2}{2E_{\mathbf{k}_2}(2\pi)^3} \frac{f^{NN}(\boldsymbol{\kappa}_\perp)}{k_1'^2 - M_N^2 + i\varepsilon} \left\langle s_1, s_2 | \Psi_D^{\mathcal{M}_2}(\mathbf{p}_m) \right\rangle \right|^2 = \\ &= \sum_{\mathcal{M}_2, s_1, s_2} \left| \mathcal{T}_D^{(0)}(\mathcal{M}_2, s_1, s_2) + \mathcal{T}_D^{(1)}(\mathcal{M}_2, s_1, s_2) \right|^2 \end{aligned} \quad (48)$$

and the quantities

$$\mathcal{T}_D^{(0)}(\mathcal{M}_2, s_1, s_2) = \left\langle s_1, s_2 | \Psi_D^{\mathcal{M}_2}(\mathbf{k}_2) \right\rangle \quad (49)$$

and

$$\mathcal{T}_D^{(1)}(\mathcal{M}_2, s_1, s_2) = \int \frac{d^3k_2}{2E_{\mathbf{k}_2}(2\pi)^3} \frac{f^{NN}(\boldsymbol{\kappa}_\perp)}{k_1'^2 - M_N^2 + i\varepsilon} \left\langle s_1, s_2 | \Psi_D^{\mathcal{M}_2}(\mathbf{p}_2) \right\rangle \quad (50)$$

can be called the *reduced (Lorentz index independent) amplitudes*; in the above equations the deuteron wave function $\Psi_D^{\mathcal{M}_2}$ is given by Eq. (19) and the spin wave function refers to the two particles in the continuum.

To sum up we have shown that:

1. the cross section which includes FSI factorizes provided: i) the spin flip part of the NN scattering amplitude can be disregarded, which is consistent with the high energies we

are considering, and ii) the momentum transfer κ in the NN rescattering is small and transverse, so that in the integral (43) one has $\mathbf{k}_2 \sim \mathbf{p}_2$ or, equivalently, $\mathbf{k}_2 \simeq \mathbf{p}_m$; this is a reasonable approximation, thanks to the behaviour of the elastic NN scattering amplitude, which is sharply peaked in the forward direction;

2. in the eikonal approximation and neglecting the spin dependence (spin-flip part) of the NN -amplitude, the FSI is not affected by the spin structure of the wave functions of the deuteron and the two-body final state. This means that in computing the Feynman diagrams, the intermediate spin algebra can be disregarded, and only the scalar part of the corresponding vertex functions can be considered, using Eq. (35) to define the scalar parts of the wave functions. Then the resulting amplitude has to be merely sandwiched between the spin functions of initial and final particles.

The above conclusions can be generalized to a nucleus A , obtaining for the cross section of the process $A(e, e'p)(A - 1)$ the following expression

$$\frac{d^6\sigma}{dE'd\Omega'd\mathbf{p}_m} = K(\bar{Q}^2, x, \mathbf{p}_m) \sigma^{eN}(\bar{Q}^2, \mathbf{p}_m) P_A^{FSI}(\mathbf{p}_m, E_m) \quad (51)$$

where $P_A^{FSI}(\mathbf{p}_m, E_m)$ is the *Distorted Spectral Function*

$$\begin{aligned} P_A^{FSI}(\mathbf{p}_m, E_m) &= \frac{1}{(2\pi)^3} \frac{1}{2J_A + 1} \sum_f \sum_{\mathcal{M}_A, \mathcal{M}_{A-1}, s_1} \left| \sum_{n=0}^{A-1} \mathcal{T}_A^{(n)}(\mathcal{M}_2, \mathcal{M}_{A-1}, s_1) \right|^2 \times \\ &\times \delta(E_m - (E_{A-1}^f + E_{min})) \end{aligned} \quad (52)$$

and n denotes the order of rescattering. In what follows the distorted momentum distributions for the Deuteron (Eq. (48)) and the distorted Spectral Function for 3He (Eq. (52)) will be calculated within the GA and GGA approximations.

B. The process ${}^2H(e, e'p)n$ within the GA and GGA.

Let us now calculate the reduced amplitude $\mathcal{T}_D^{(1)}$ in the process ${}^2H(e, e'p)n$, taking FSI into account by the GGA. This amounts to replace the energy denominator in Eq. (50) by its generalized eikonal approximation. To this end, we will consider both the "canonical" case, when the value of the 3-momenta transfers $|\mathbf{q}|$ is so high that $\mathbf{q} \simeq \mathbf{p}_1$, with the z -axis naturally directed along \mathbf{q} , as well as the case of smaller values of \mathbf{q} , but high values of \mathbf{p}_1 ,

when \mathbf{q} and \mathbf{p}_1 may point to different directions, in which case the z -axis is oriented along \mathbf{p}_1 .

Remembering that $\kappa = p_1 - k'_1 = k_2 - p_2$, the energy denominator can be written as follows

$$\begin{aligned} k'_1 - M_N^2 &= (p_1 - \kappa)^2 - M_N^2 = -2p_1\kappa + \kappa^2 = \\ &= 2|\mathbf{p}_1| \left(\kappa_z + \frac{\kappa_0(\kappa_0 - 2E_{\mathbf{p}_1})}{2|\mathbf{p}_1|} - \frac{\kappa^2}{2|\mathbf{p}_1|} \right) \approx \\ &\approx 2|\mathbf{p}_1| \left(\kappa_z - \frac{E_{\mathbf{k}_1+\mathbf{q}} + E_{\mathbf{p}_1}}{2|\mathbf{p}_1|} \kappa_0 \right) \approx \\ &\approx 2|\mathbf{p}_1| (\kappa_z + \Delta_z) \end{aligned} \quad (53)$$

where

$$\Delta_z = \frac{E_{\mathbf{k}_1+\mathbf{q}} + E_{\mathbf{p}_1}}{2|\mathbf{p}_1|} (E_m - |E_A|) \quad (54)$$

and the relation

$$\kappa_0 = E_{\mathbf{p}_1} - E_{\mathbf{k}_1+\mathbf{q}} \approx -(E_m - |E_A|) \quad (55)$$

resulting from energy conservation $q_0 + M_A = E_{\mathbf{p}_1} + E_{\mathbf{p}_2}$ has been used.

By changing the normalization of the NN amplitude from the covariant one to the non relativistic analogue ($E_{\mathbf{p}} \simeq M_N$), one has

$$\frac{f^{NN}(\kappa_{\perp})}{4E_{\mathbf{p}}|\mathbf{p}_1|} \approx \frac{f^{NN}(\kappa_{\perp})}{4M_N|\mathbf{p}_1|} = a^{NR}(\kappa_{\perp}) \equiv i \int d^2\mathbf{b} e^{i\kappa_{\perp}\mathbf{b}} \Gamma(\mathbf{b}) \quad (56)$$

and $\mathcal{T}_D^{(1)}$ becomes.

$$\mathcal{T}_D^{(1)}(\mathcal{M}_2, s_1, s_2) = \int \frac{d^3k}{(2\pi)^3} a^{NR}(\kappa_{\perp}) \frac{1}{\kappa_z + \Delta_z + i\varepsilon} \langle s_1, s_2 | \Psi_D^{\mathcal{M}_2}(\mathbf{p}) \rangle \quad (57)$$

Using

$$\frac{1}{\kappa_z + \Delta_z + i\varepsilon} = -i \int \theta(z) e^{i(\kappa_z + \Delta_z) \cdot z} dz \quad (58)$$

we obtain, in coordinate space,

$$\mathcal{T}_D^{(0)}(\mathcal{M}_2, s_1, s_2) + \mathcal{T}_D^{(1)}(\mathcal{M}_2, s_1, s_2) = \left\langle s_1, s_2 \left(1 - \theta(z) e^{i\Delta_z z} \Gamma(\mathbf{b}) \right) e^{-i\mathbf{p}_m \mathbf{r}} | \Psi_D^{\mathcal{M}_2}(\mathbf{r}) \right\rangle \quad (59)$$

As a result, the cross section will read as follows

$$\frac{d^6\sigma}{dE'd\Omega'd\mathbf{p}_m} = K(\bar{Q}^2, x, \mathbf{p}_m) \sigma^{eN}(\bar{Q}^2, \mathbf{p}_m) n_D^{FSI}(\mathbf{p}_m) \delta(M_D + \nu - E_{\mathbf{p}_1} - E_{\mathbf{p}_m}) \quad (60)$$

with the *distorted momentum distributions* n_D^{FSI} defined by

$$n_D^{FSI}(\mathbf{p}_m) = \frac{1}{3} \frac{1}{(2\pi)^3} \sum_{\mathcal{M}_D, S_{23}} \left| \int d\mathbf{r} \chi_{S_{23}}^\dagger(\mathbf{r}) \Psi_D^{\mathcal{M}_2\dagger}(\mathbf{r}) \mathcal{S}_\Delta^{FSI}(\mathbf{r}) \exp(-i\mathbf{p}_m \mathbf{r}) \right|^2, \quad (61)$$

where $\mathcal{S}_\Delta^{FSI}(\mathbf{r})$, which describes the final state interaction between the hit nucleon and the spectator, is

$$\mathcal{S}_\Delta^{FSI}(\mathbf{r}) = 1 - \theta(z) e^{i\Delta_z z} \Gamma(\mathbf{b}) \quad (62)$$

with $\mathbf{r} = (\mathbf{b}, z)$. In the above formulae the z-axis is along \mathbf{p}_1 ; it should be pointed out, however, that at large values of the momentum transfer, the hit nucleon propagates almost along \mathbf{q} so that by choosing the z-axis along the three-momentum transfer and neglecting the virtuality of the struck nucleon before and after interaction, one can write [10]

$$k_1'^2 - M_N^2 = (k_1 + q)^2 - M_N^2 \approx 2|\mathbf{q}|(\kappa_z + \Delta_z) \quad (63)$$

where

$$\Delta_z = \frac{q_0}{|\mathbf{q}|} E_m \quad (64)$$

It can be seen that the FSI factor (62) in the GGA differs from the one of the standard GA [42, 43, 44], simply for the additional factor $e^{i\Delta_z z}$. It should be pointed out that whereas the well known factor $\theta(z)$ [43, 44] originates from the non relativistic reduction of the covariant Feynman diagrams and guarantees the correct time ordering of the rescattering processes, the quantity Δ_z is of a pure nuclear structure origin and, as it can be seen from Eq. (59), it represents a correction to the parallel component of the missing momentum. Therefore the

corrections from Δ_z are expected to be important in the parallel kinematics at $|\mathbf{p}_z| \simeq \Delta_z$. As we shall see from the results of our calculations, performed in perpendicular kinematics in the range with $|\mathbf{p}_m| \leq 600 \text{ MeV}/c$ and $E_m \leq 100 \text{ MeV}$, one always has $|\Delta_z| \ll |\mathbf{p}|_\perp$ with $q_0/|\mathbf{q}| \simeq 1$, so that Δ_z is always very small. We can therefore anticipate that effects of Δ_z on the experimental data we have considered is also very small.

C. The processes ${}^3H(e, e'p){}^2H$ and ${}^3H(e, e'p)(np)$ within the GA and GGA.

Let us now consider the three-body system. The distorted Spectral Function is given by Eq. (52)

$$P_{He}^{FSI}(\mathbf{p}_m, E_m) = \frac{1}{(2\pi)^3} \frac{1}{3} \sum_f \sum_{\mathcal{M}_3, \mathcal{M}_2, s_1} \left| \sum_{n=0}^2 \mathcal{T}_A^{(n)}(\mathcal{M}_3, \mathcal{M}_2, s_1) \right|^2 \times \delta(E_m - (E_2^f + E_{min})) \quad (65)$$

where the magnetic quantum number \mathcal{M}_2 refers either to the deuteron or to the two nucleon in the continuum, depending upon the break-up channel we are considering ($E_{min} = E_3 - E_2$ ($E_{min} = E_3$) for the two-body (three-body) break-up channel). The diagrams representing the rescattering processes are shown in Fig. 6. The evaluation of these diagrams follows the standard procedure adopted for the deuteron. Let us illustrate it in the case of the 3bbu considering, for ease of presentation, the single scattering diagram of Fig. 6 b). After integration over k_{20} and k_{30} in the corresponding poles of the propagators of the spectators ($k_{20} = E_{\mathbf{k}_2}$ and $k_{30} = E_{\mathbf{k}_3}$), we obtain

$$\mathcal{T}_3^{(1)}(\mathcal{M}_3, s_1, s_2, s_3) = \int \frac{d^3 k_2}{2E_{\mathbf{k}_2}(2\pi)^3} \frac{d^3 k_3}{2E_{\mathbf{k}_3}(2\pi)^3} \times \times \frac{G_{He \rightarrow 1(23)}(k_1, k_2, k_3, s_1, s_2, s_3)}{(k_1^2 - M_N^2)} \frac{f_{NN}(p_1 - k'_1)}{k_1'^2 - M_N^2} \frac{G_{(23) \rightarrow f}^+(k'_2, k_3, s_2, s_3)}{(k'_2 - M_N^2)} \quad (66)$$

where the overlaps of the vertex functions G_i are

$$G_{He \rightarrow 1(23)}(k_1, k_2, k_3, s_1, s_2, s_3) = \langle \mathbf{k}_1, s_1, \mathbf{k}_2, s_2, \mathbf{k}_3, s_3 | G_{He \rightarrow 1(23)}(\mathcal{M}_3, \mathbf{P}_3) \rangle; \quad (67)$$

$$G_{(23) \rightarrow f}(k_2, k_3, s_2, s_3) = \langle \mathbf{k}_2, s_2, \mathbf{k}_3, s_3 | G_{(23) \rightarrow f}(\mathcal{M}_{23}, S_{23}, \mathbf{P}_2, E_2^f) \rangle; \quad (68)$$

The vertex functions G_i are replaced by the non relativistic overlap functions according to the general convention (we omit for ease of presentation the proper normalization factors)

$$\langle s_1, s_2, s_3 | \Psi_{He}^{\mathcal{M}_3}(\mathbf{k}_1, \mathbf{k}_2, \mathbf{k}_3) \rangle \approx \frac{G_{He \rightarrow 1(23)}(k_1, k_2, k_3, s_1, s_2, s_3)}{(k_1^2 - M_N^2)} \quad (69)$$

and, using the completeness relation when summing over s_2 and s_3 , one gets

$$\begin{aligned} \mathcal{T}_3^{(1)}(Q^2, s_1, S_{23}) &= \int \frac{d^3 k_2}{2E_{\mathbf{k}_2}(2\pi)^3} \frac{d^3 k_3}{2E_{\mathbf{k}_3}(2\pi)^3} \times \\ &\times \Psi_{(23)}^f(\mathbf{k}_3, \mathbf{k}'_2; S_{23}) \frac{f_{NN}(\boldsymbol{\kappa})}{(k_1'^2 - M_N^2 + i\epsilon)} \langle s_1 | \Psi_{He}^{\mathcal{M}_3}(\mathbf{k}_1, \mathbf{k}_2, \mathbf{k}_3) \rangle \end{aligned} \quad (70)$$

Following the procedure adopted for the deuteron, we obtain

$$\begin{aligned} \mathcal{T}_3^{(1)}(Q^2, s_1, S_{23}) &= \\ &= \int \frac{d^3 \kappa}{(2\pi)^3 2E_{\mathbf{k}_2}} \Psi_{(23)}^f(\mathbf{k}_3, \mathbf{k}'_2; S_{23}) \frac{f_{NN}(\boldsymbol{\kappa})}{k_1'^2 - M_N^2 + i\epsilon} \langle s_1 | \Psi_{He}^{\mathcal{M}_3}(\mathbf{k}_1, \mathbf{k}_2, \mathbf{k}_3) \rangle \approx \\ &\approx \int \frac{d^3 \kappa}{(2\pi)^3} \Psi_{(23)}^f(\mathbf{k}_3, \mathbf{k}'_2; S_{23}) \frac{f_{NN}(\boldsymbol{\kappa})/4M_N|\mathbf{p}_1|}{(\kappa_z + \Delta_z + i\epsilon)} \langle s_1 | \Psi_{He}^{\mathcal{M}_3}(\mathbf{k}_1, \mathbf{k}_2, \mathbf{k}_3) \rangle \end{aligned} \quad (71)$$

where

$$\Delta_z = \frac{E_{\mathbf{k}_1 + \mathbf{q}} + E_{\mathbf{p}_1}}{2|\mathbf{p}_1|} (E_m - E_3) \quad (72)$$

Including also the 2buu channel, we can write, in coordinate space,

$$P_{He}^{FSI}(\mathbf{p}_m, E_m) = P_{gr}^{FSI}(\mathbf{p}_m, E_m) + P_{ex}^{FSI}(\mathbf{p}_m, E_m), \quad (73)$$

where

$$P_{gr}^{FSI}(\mathbf{p}_m, E_m) = n_{gr}^{FSI}(\mathbf{p}_m) \delta(E_m - (E_3 - E_2)) \quad (74)$$

with

$$n_{gr}^{FSI}(\mathbf{p}_m) = \frac{1}{(2\pi)^3} \frac{1}{2} \sum_{\mathcal{M}_3, \mathcal{M}_2, s_1} \left| \int e^{i\boldsymbol{\rho}\mathbf{p}_m} \chi_{\frac{1}{2}s_1}^\dagger(\mathbf{r}) \Psi_D^{\mathcal{M}_2 \dagger}(\mathbf{r}) \mathcal{S}_\Delta^{FSI}(\boldsymbol{\rho}, \mathbf{r}) \Psi_{He}^{\mathcal{M}_3}(\boldsymbol{\rho}, \mathbf{r}) d\boldsymbol{\rho} d\mathbf{r} \right|^2 \quad (75)$$

and

$$P_{ex}^{FSI}(\mathbf{p}_m, E_m) = \frac{1}{(2\pi)^3} \frac{1}{2} \sum_{\mathcal{M}_3, S_{23}, s_1} \int \frac{d^3 \mathbf{t}}{(2\pi)^3} \left| \int e^{i\boldsymbol{\rho} \mathbf{p}_m} \chi_{\frac{1}{2} s_1}^\dagger(\mathbf{r}) \mathcal{S}_\Delta^{FSI}(\boldsymbol{\rho}, \mathbf{r}) \Psi_{He}^{\mathcal{M}_3}(\boldsymbol{\rho}, \mathbf{r}) \boldsymbol{\rho} d\boldsymbol{\rho} d\mathbf{r} \right|^2 \times \delta \left(E_m - \frac{\mathbf{t}^2}{M_N} - E_3 \right), \quad (76)$$

The FSI factor \mathcal{S}_Δ^{FSI} describes the single and double rescattering of nucleon "1" with the spectators "2" and "3", and has the following form

$$\mathcal{S}_\Delta^{FSI}(\boldsymbol{\rho}, \mathbf{r}) = \mathcal{S}_{(1)}^{FSI}(\boldsymbol{\rho}, \mathbf{r}) + \mathcal{S}_{(2)}^{FSI}(\boldsymbol{\rho}, \mathbf{r}) \quad (77)$$

with the single scattering contribution $\mathcal{S}_{(1)}^{FSI}$ given by

$$\mathcal{S}_{(1)}^{FSI}(\boldsymbol{\rho}, \mathbf{r}) = 1 - \sum_{i=2}^3 \theta(z_i - z_1) e^{i\Delta_z(z_i - z_1)} \Gamma(\mathbf{b}_1 - \mathbf{b}_i) \quad (78)$$

and the double scattering contribution by (Ref. [10])

$$\begin{aligned} \mathcal{S}_{(2)}^{FSI}(\boldsymbol{\rho}, \mathbf{r}) &= \\ &= \left[\theta(z_2 - z_1) \theta(z_3 - z_2) e^{-i\Delta_3(z_2 - z_1)} e^{-i(\Delta_3 - \Delta_z)(z_3 - z_1)} + \right. \\ &\quad \left. + \theta(z_3 - z_1) \theta(z_2 - z_3) e^{-i\Delta_2(z_3 - z_1)} e^{-i(\Delta_2 - \Delta_z)(z_2 - z_1)} \right] \times \\ &\quad \times \Gamma(\mathbf{b}_1 - \mathbf{b}_2) \Gamma(\mathbf{b}_1 - \mathbf{b}_3) \end{aligned} \quad (79)$$

where $\Delta_i = (q_0/|\mathbf{q}|)(E_{\mathbf{p}_i} - E_{\mathbf{k}'_i})$ and Δ_z is given by Eq. (64).

When $\Delta_z = 0$, the familiar form for \mathcal{S}^{FSI} is obtained, namely

$$\mathcal{S}^{FSI}(\boldsymbol{\rho}, \mathbf{r}) = \prod_{i=2}^3 [1 - \theta(z_i - z_1) \Gamma(\mathbf{b}_i - \mathbf{b}_1)], \quad (80)$$

and when $\Gamma = 0$, the distorted Spectral Function (73) transforms into the usual Spectral Function (21).

Using Eq. (73), the cross section of the process ${}^3He(e, e'p)X$ ($X = D$ or (np)) assumes the following form

$$\frac{d^6 \sigma}{dE' d\Omega' d\mathbf{p}_m} = K(\bar{Q}^2, x, \mathbf{p}_m) \sigma^{eN}(\bar{Q}^2, \mathbf{p}_m) P_{He}^{FSI}(\mathbf{p}_m, E_m). \quad (81)$$

V. RESULTS OF THE CALCULATIONS

We have used Eqs. (60), (62), (81) and (79) to calculate the cross sections of the processes $^2H(e, e'p)n$, $^3He(e, e'p)^2H$ and $^3He(e, e'p)(np)$. All calculations have been performed using the following well known parametrization of the profile function $\Gamma(\mathbf{b})$

$$\Gamma(\mathbf{b}) = \frac{\sigma_{NN}^{tot}(1 - i\alpha_{NN})}{4\pi b_0^2} e^{-\mathbf{b}^2/2b_0^2}, \quad (82)$$

where σ_{NN}^{tot} is the total NN cross section, α_{NN} the ratio of the real to imaginary part of the forward NN amplitude, and b_0 the slope of the differential elastic NN cross section. The values of the energy dependent quantities σ_{NN}^{tot} and α_{NN} have been taken from Ref. [45]. For the electron-nucleon cross section $\sigma^{eN}(\bar{Q}^2, \mathbf{p}_m)$ we used the De Forest $\sigma_{cc1}^{eN}(\bar{Q}^2, \mathbf{p}_m)$ cross section [31]. All two-and three-body wave functions are direct solutions of the non relativistic Schrödinger equation, therefore our calculations are fully parameter free.

Calculations have been performed in PWIA and including the full rescattering within the GA and the GGA approximations by evaluating the Feynman diagrams shown in Figs. 5 and 6.

A. The process $^2H(e, e'p)n$

Our results for the process $^2H(e, e'p)n$ are compared in Figs. 6, 7 and 8 with three different sets of experimental data, covering different kinematical ranges, namely the experimental data from NIKHEF [16], SLAC [18], and Jlab [17].

In Figs. 7 and 9 theoretical cross section corresponding to Eq. (60), namely

$$\frac{d^5\sigma}{dE'd\Omega'd\Omega_{\mathbf{p}_m}} = f_{rec} \mathcal{K}(Q^2, x, \mathbf{p}_m) \sigma_{cc1}^{eN}(\bar{Q}^2, \mathbf{p}_m) n_D^{FSI}(\mathbf{p}_m) \quad (83)$$

is compared with the corresponding data, whereas in Fig. 8 we compare, as in Ref. [17], the effective momentum distributions $N_{eff}(p_m)$ (or reduced cross section) defined by [17]

$$N_{eff}(|\mathbf{p}_m|) = \frac{d^5\sigma^{exp}}{d\Omega'dE'd\Omega_{\mathbf{p}_m}} \left[f_{rec} \mathcal{K} \sigma_{cc1}^{eN} \right]^{-1} \quad (84)$$

where in Eqs. (83) and (84) f_{rec} and \mathcal{K} are kinematical factors which arise from the integration over $dT_{\mathbf{p}_1}$. The relevant kinematical variables in the experiment of Ref. [17] ,

performed in perpendicular kinematics, are $Q^2 \simeq 0.665 \text{ (GeV}/c)^2$, $|\mathbf{q}| \simeq 0.7 \text{ GeV}/c$, and $x \simeq 0.96$. As for the NIKHEF and SLAC experiments, the relevant kinematical quantities are $0.1 \leq Q^2 \leq 0.3$, $0.3 \leq x \leq 0.6$ and $1.2 \leq Q^2 \leq 6.8$, $x \simeq 1$, respectively. The results presented in Figs. 7, 8 and 9 exhibit a general satisfactory agreement between theoretical calculations and experimental data, particularly in view of the wide range of kinematics covered by the data we have considered. Figs. 8 and 9 show however that quantitative disagreements with data exist in some regions. Particularly worth being noted is the disagreement in the region around $|\mathbf{p}_m| \simeq 0.25 \text{ GeV}/c$ appearing in Fig. 8. We did not try to remove such a disagreement by adjusting the quantities entering the profile function (60), but it turns out that n_D^{FSI} in the region around $|\mathbf{p}_m| \simeq 0.25 \text{ GeV}/c$ is rather sensitive to the value of α . The results of the GA and GGA differs by only few percent and cannot be distinguished in the Figures. The effects of MEC and Δ isobar production has been investigated in Ref. [18] and found to be small ($\simeq 5 - 6\%$) in that kinematics; the results from [16] and [53], show the same trend also in the NIKHEF and Jlab results.

B. The processes ${}^3He(e, e'p){}^2H$ and ${}^3He(e, e'p)(np)$.

Calculations for the three-body systems are very involved, mainly because of the complex structure of the wave function of Ref. [2], which is given in a mixed $(L_\rho, X, j_{23}, S_{23})$ representation, including angular momentum values up to $L_\rho = 7$ and $j_{23} = 8$ (a total of 58 configurations with different combinations of $(L_\rho, X, j_{23}, S_{23})$ quantum numbers). Correspondingly, the wave function of the spectators (the deuteron or the continuum two-nucleon states) is given in a *JLS*-scheme (see Appendix A). We would like to stress, that no approximations have been made in the evaluation of the single and double scattering contributions to the FSI: proper intrinsic coordinates have been used and the energy dependence of the profile function has been taken into account in the properly chosen CM system of the interacting pair. The Feynman diagrams which have to be evaluated, both for the 2bbu and 3bbu channels are shown in Fig. 6.

1. *The two-body break-up channel ${}^3He(e, e'p){}^2H$.*

The 2bbu channel cross section

$$\frac{d^5\sigma}{dE'd\Omega'd\Omega_{\mathbf{p}_1}} = K_{2bbu}(\bar{Q}^2, x, \mathbf{p}_m) \sigma_{ccl}^{eN}(\bar{Q}^2, \mathbf{p}_m) n_{gr}^{FSI}(\mathbf{p}_m) \quad (85)$$

obtained from Eq. (81), with $n_{gr}^{FSI}(\mathbf{p}_m)$ given by Eq. (75), is compared in Fig. 10 with preliminary experimental data from the E89044 Jlab Collaboration [21]. The relevant kinematical variables in the experiment are $|\mathbf{q}| = 1.5 \text{ GeV}/c$, $q_0 = 0.84 \text{ GeV}$, $Q^2 = 1.55 \text{ (GeV}/c)^2$, and $x \approx 1$. The cross section is presented as a function of the missing momentum $|\mathbf{p}_m|$ (which, for the ${}^3He(e, e'p){}^2H$ process, exactly coincides with the final deuteron momentum). In PWIA the cross section is directly proportional to n_{gr} (Eq. (23)) shown in the left panel of Fig. 3. It can be seen that up to $|\mathbf{p}_m| \sim 400 \text{ MeV}/c$, the PWIA and FSI results are almost the same and fairly well agree with the experimental data, which means, in turn, that the 2bbu ${}^3He(e, e'p){}^2H$ does provide information on n_{gr} ; on the contrary, at larger values of $|\mathbf{p}_m| \geq 400 \text{ MeV}/c$ the PWIA appreciably underestimates the experimental data. It is very gratifying to see that when FSI is taken into account, the disagreement is fully removed and an overall very good agreement between theoretical predictions and experimental data is obtained. It should be pointed out that the experimental data shown in Fig. 10 correspond to the perpendicular kinematics, when the deuteron momentum (the missing momentum) is always almost perpendicular to the momentum transfer \mathbf{q} ; in such a kinematics the effects from FSI are maximized, whereas in the so called parallel kinematics, they are minimized (see, e.g. [9], [44], [46]). The kinematics therefore reflects itself in the relevance of the calculated FSI; as a matter of fact, we have found that the effects of the FSI calculated either within the GA or GGA approximations, differ only by a few percent, which was expected in view of the observation that the factor Δ_z (Eqs. (72) or (64)) affects only the longitudinal component of \mathbf{p}_m and therefore has minor effects on the data we have considered. The effects of MEC and Δ isobar contributions have been estimated in [53] and found negligible up to about $p_m \simeq 600 \text{ MeV}/c$.

2. *The three-body break-up channel ${}^3He(e, e'p)(np)$.*

From Eq. (81), we obtain the cross section for the 3bbu in the following form

$$\frac{d^6\sigma}{dE'd\Omega'd\Omega_{\mathbf{p}_1}dE_m} = K_{3bbu}(\bar{Q}^2, x, \mathbf{p}_m) \sigma_{cc1}^{eN}(\bar{Q}^2, \mathbf{p}_m) P_{ex}^{FSI}(\mathbf{p}_m, E_m) \quad (86)$$

where $P_{ex}^{FSI}(\mathbf{p}_m, E_m)$ is given by Eq. (76). We have calculated Eq. (86) in correspondence of two different kinematical ranges: the one from Ref. [19] and the one corresponding to preliminary experimental data from the *E89044* Jlab Collaboration [21]. Contrary to the 2bbu channel, the 3bbu cross section depends upon an extra kinematical variable, the removal energy E_m , and corresponds to the process in which three particles interact in the continuum. We will consider three different theoretical calculations, namely:

1. the Plane Wave Approximation (PWA), when FSI effects are completely ignored , i.
e. the three particles in the continuum are described by plane waves;
2. the already introduced Plane Wave Impulse Approximation (PWIA), in which the struck nucleon is described in the continuum by a plane wave and the spectator pair is described by the continuum solution of the Schrödinger equation (obviously, in the case of the deuteron the PWIA coincides with the PWA);
3. the full FSI, when the struck nucleon interacts in the continuum with the nucleons of the spectator pair via the standard GA or the more refined GGA.

In Fig. 11 the results of our calculations are compared with the experimental data from Ref. [19]. In the experiment, which corresponds to a relatively low beam energy ($E = 0.560 \text{ GeV}$), the scattering angle ($\theta_e = 25^\circ$) and the energy transfer ($q_0 = 0.32 \text{ GeV}$) were kept constant, and protons with different values of the missing momentum and energy were detected in correspondence of several values of the proton emission angle $\theta_{\mathbf{p}_1}$, *viz* $\theta_{\mathbf{p}_1} = 45^\circ, 60^\circ, 90.5^\circ, 112^\circ$ and 142.5° . The kinematics is far from the quasi elastic peak ($x \simeq 0.1$) and the values of the four- and three-momentum transfers are low ($Q^2 \simeq 0.03 \text{ (GeV/c)}^2$ and $|\mathbf{q}| = 0.28 \text{ GeV/c}$). At first glance this would invalidate the use of the eikonal approximation; however, a detailed analysis of the kinematics, shows that the value of both \mathbf{p}_1 and \mathbf{p}_m are rather large ($400 - 600 \text{ MeV/c}$), and so is the value of the angle between them ($\widehat{\theta_{\mathbf{p}_1 \mathbf{p}_m}} \sim 150^\circ$); thus the momentum of the struck nucleon relative to the spectator pair is high enough to make the use of the eikonal approximation justified. Moreover, the values of the experimentally measured missing momenta and missing energy

at each value of $\theta_{\mathbf{p}_1}$, always cover the kinematical range where the condition for two nucleon correlation mechanism $E_m \sim \frac{\mathbf{p}_m^2}{4M_N}$ holds; as a matter of fact, as it can be seen from Fig. 11, the position of the bumps in the cross section are reasonably predicted by the PWA and PWIA.

The results presented in Fig. 11 clearly show that with increasing missing momentum, the experimental peak moves to higher values of missing energy, in qualitative agreement with the two-nucleon correlation mechanism. More important, it can be seen that at the highest value of $|\mathbf{p}_m|$ ($\theta_{\mathbf{p}_1} = 112^\circ$) the effects of FSI, both in the spectator pair and between the struck nucleon and the spectator pair, is very small. This is because the kinematics of the experiment is not purely perpendicular: the relation between $|\mathbf{p}_{m\perp}|$ and $|\mathbf{p}_m|$ is such that $|\mathbf{p}_{m\perp}| \sim \frac{1}{2}|\mathbf{p}_m|$, so that the dominant role played by FSI in the purely perpendicular kinematics is decreased with increased values of $\theta_{\mathbf{p}_1}$.

In Fig. 12 our results are compared with the preliminary data from the Jlab E89044 Collaboration, where the cross section was measured at fixed values $|\mathbf{p}_m|$ *vs.* the missing energy E_m . As in the case of the Saclay data previously analyzed, even in this case the cross section exhibits bumps approximately located at values of E_m and $|\mathbf{p}_m|$ satisfying the two-nucleon correlation mechanism relation ($E_m \sim \frac{\mathbf{p}_m^2}{4M_N}$), and in agreement with the behaviour of the Spectral Function (see Figs.3 and 4). However, contrary to the Saclay case, the PWIA dramatically underestimates the experimental data. This is clear evidence that the FSI between the struck nucleon and the nucleons of the spectator pair (Feynman diagrams b) and c) in Fig. 6) does play a relevant role, as the results of our calculations (the full line in Fig. 12) do indeed really show. Since, as already stressed, the Jlab experiment correspond to a perpendicular kinematics, this explains the larger effects of the FSI with respect to the Saclay experiment. The effects of the FSI calculated either within the GA or GGA approximations, differ only by a few percent, which was expected in view of the observation that the factor Δ_z (Eqs. (72) or (64)) affects only the longitudinal component of \mathbf{p}_m and therefore has minor effects on the data we have considered. The effects of MEC and Δ , calculated by the approach by Laget (see [21]), appear to reduce the cross section in the peak by about 10%.

VI. SUMMARY AND CONCLUSIONS

We have calculated the cross section of the processes $^2H(e, e'p)n$, $^3He(e, e'p)D$, and $^3He(e, e'p)(np)$, using realistic wave functions for the ground state, exhibiting the rich correlation structure generated by modern NN interactions, and treating the FSI of the struck nucleon with the spectator nucleons within the standard Glauber eikonal approximation (GA) [15], as well as with its generalized version (GGA) [9, 10, 11]. The two approaches differ by a factor Δ_z (Eqs. (54) and (64)) which modifies (see Eq. (77)) the FSI factor appearing in the standard GA (Eq. (80)). This factor takes into account in the NN scattering amplitude the removal energy of the struck nucleon, or, equivalently, the excitation energy of the system $A - 1$. By properly choosing the z -axis (along \mathbf{q} or \mathbf{p}_1), we were able to calculate FSI effects either in the case of large values of the three-momentum transfer \mathbf{q} , or large values of the momentum of the struck nucleon \mathbf{p}_1 relative to the $A - 1$ system; by this way calculations could be extended successfully even at relatively low values of Q^2 . As far as the three-body break-up channel in 3He is concerned, the FSI in the spectator pair was always calculated by the solution of the Schrödinger equation (PWIA), whereas the interaction of the active, fast nucleon with the two nucleons of the spectator pair has been taken care of by the GA or GGA approximations. The method we have used is a very transparent one and fully parameter free: it is based upon Eqs. (61), (73), and (77) which only require the knowledge of the nuclear wave functions, since the FSI factor is fixed directly by the NN scattering data. Of course with increasing A , the order of rescattering increases up to the $(A - 1)$ -th order; we have performed calculations in the three-body case exactly, and did not investigate the problem of the convergence of the multiple scattering series. This problem is under investigation in the case of 4He . Most of our calculations have been performed in kinematical conditions ($x \simeq 1$) where the effects of MEC, Δ isobar creation, etc. is expected to be minimized, as calculations of the same quantities we have considered performed by other authors , but including MEC and Δ isobars, indeed show [47, 48, 49, 50, 51, 52, 53].

As for the main results we have obtained , the following remarks are in order:

1. the agreement between the results of our calculations and the experimental data for both the deuteron and 3He , is a very satisfactory one, particularly in view of the lack of any adjustable parameter in our approach;

2. the effects of the FSI are such that they systematically bring theoretical calculations in better agreement with the experimental data. For some quantities, FSI simply improve the agreement between theory and experiment (cf. e.g. Figs. 7, 9 and 11), whereas for some other quantities, they play a dominant role (see e.g. Fig. 10 and 12);
3. a comparison of the PWA and the PWIA with the full FSI calculation, does show that proper kinematics conditions could be found corresponding to an overall very small effect from FSI, leaving thus room for the investigation of the details of the nuclear wave function; as a matter of fact, we always found that in the 3bbu channel in 3He , $^3He(e, e'p)(np)$, the experimental values of p_m and E_m corresponding to the maximum values of the cross section, satisfy to a large extent the relation predicted by the two-nucleon correlation mechanism [34], namely $E_m \simeq p_m^2/4M_N + E_3$ (cf. Fig. 3, right panel), with the full FSI mainly affecting only the magnitude of the cross section;
4. calculations of the 2bbu channel disintegration of 4He , i.e. the process $^4He(e, e'p)^3H$, have already been performed [14] using realistic wave functions and taking exactly into account nucleon rescattering up to 3rd order, i.e by using the generalization of Eq. (77) to the four-particle case, *viz*

$$\mathcal{S}_\Delta^{FSI} = \mathcal{S}_{(1)}^{FSI}(\mathbf{R}, \mathbf{r}_{12}, \mathbf{r}_{34}) + \mathcal{S}_{(2)}^{FSI}(\mathbf{R}, \mathbf{r}_{12}, \mathbf{r}_{34}) + \mathcal{S}_{(3)}^{FSI}(\mathbf{R}, \mathbf{r}_{12}, \mathbf{r}_{34}) \quad (87)$$

where \mathbf{R} , \mathbf{r}_{12} , and \mathbf{r}_{34} are four-body Jacobi coordinates. Calculations for the 3bbu and 4bbu channels are in progress and will be reported elsewhere [54]; they should in principle yield results appreciably differing from the predictions based upon shell-model type four-body wave functions;

5. our results are generally of the same quality of the ones performed by different authors, so it would appear that the problem of the treatment of FSI at high values of Q^2 (or high \mathbf{p}_1) is under control; nevertheless, a systematic comparison of the various approaches would be highly desirable;
6. eventually, it appears that in the kinematical range we have considered only minor numerical differences were found between the conventional Glauber-eikonal approach and its generalized extension; this does not mean at all that the same will hold in other kinematical conditions (see e.g. [9, 10, 11]).

VII. ACKNOWLEDGMENTS

The authors are indebted to A. Kievsky for making available the variational three-body wave functions of the Pisa Group and to G. Salmè for useful discussions about their use. Thanks are due to M.A. Braun and D. Treleani for stimulating discussions on the Feynman diagram approach to nucleon rescattering.

Many useful discussions with various members of the Jlab Experiment E-89-044 are gratefully acknowledged. We express our gratitude to M. Alvioli for a careful reading of the manuscript. L.P.K. is indebted to the University of Perugia and INFN, Sezione di Perugia, for a grant and for warm hospitality. This work was partially supported by the Italian Ministero dell'Istruzione, Università e Ricerca (MIUR), through the funds COFIN01, and by the Russian Fund for Basic Research 00-15-96737.

APPENDIX A: THE NUCLEAR WAVE FUNCTIONS

In our calculations we have used two- and three-body wave functions corresponding to the *AV18* potential [5].

1. The ground state wave function of 3He

For the 3He wave function we have adopted the correlated variational wave function by the Pisa group [2] which is written in a mixed $(L_\rho, X, j_{23}, S_{23})$ -representation, where j_{23} and S_{23} are the total angular momentum and the total spin of the pair "23", X is an intermediate angular momentum resulting from the coupling $\mathbf{j}_{23} + \mathbf{s}_1$ and L_ρ is the radial angular momentum of the motion of the nucleon "1" relative to the pair "23". The explicit form of the wave function is

$$\Psi_3^{M_{He}}(\boldsymbol{\rho}, \mathbf{r}) = \sum_{\{\alpha\}} \sum_{\{m\}} \langle XM_X \ L_\rho m_\rho | \frac{1}{2} M_{He} \rangle \langle j_{23} m_{23} \ \frac{1}{2} \sigma_1 | XM_X \rangle \chi_{\frac{1}{2} \sigma_1} Y_{L_\rho M_\rho}(\hat{\boldsymbol{\rho}}) \langle l_{23} \mu_{23} \ S_{23} \nu_{23} | j_{23} m_{23} \rangle Y_{l_{23} \mu_{23}}(\hat{\mathbf{r}}) \chi_{S_{23} \nu_{23}} R_{\{\alpha\}}(r, \rho) \mathcal{I}_{\frac{1}{2} \frac{1}{2}}^{T_{23}}, \quad (A1)$$

where $\{\alpha\}$ labels all possible configurations in 3He with quantum numbers $L_\rho, X, j_{23}, S_{23}$, and T_{23} and $\langle l_1 m_1 l_2 m_2 | l_{12} m_{12} \rangle$ is a Clebsch-Gordan coefficient. The total isospin function

is $\mathcal{I}_{\frac{1}{2}\frac{1}{2}}^{T_{23}} = \sum \langle T_{23}\tau_{23} \frac{1}{2}\tau_1 | \frac{1}{2}\frac{1}{2} \rangle \mathcal{J}_{T_{23}\tau_{23}} \eta_{\frac{1}{2}\tau_1}$, where $\mathcal{J}_{T_{23}\tau_{23}}$ and $\eta_{\frac{1}{2}\tau_1}$ are the isospin functions of the pair and the nucleon, respectively. Obviously, because of Pauli principle and parity constraints, the allowed configurations in eq. (A1) are those which satisfy the following conditions:

$$L_\rho + l_{23} - \text{even} \quad \text{and} \quad l_{23} + S_{23} + T_{23} - \text{odd} \quad (\text{A2})$$

The corresponding radial part of the wave function, $R_{\{\alpha\}}(r, \rho)$, has been obtained [2] by a variational method using the *AV18* potential including into the calculations values of $L_\rho, l_{12} = 0 \dots 9$ (a total of 58 different configurations $L_\rho, X, j_{23}, l_{23}, S_{23}$ have been considered).

2. The two-body continuum wave function $\Psi_{23}^t(\mathbf{r})$.

With the representation (A1) of the 3He wave function, it was convenient to adopt for the two-nucleon scattering state $\Psi_{23}^t(\mathbf{r})$ the spin-channel representation $\Psi_{S_{23}\nu_{23}}^t(\mathbf{r})$, characterized by the total (conserved in the scattering process) spin S_{23} and its projection ν_{23} . For spin $S_{23} = 1$ one has

$$\Psi_{S_f\nu_f}^t(\mathbf{r}) = 4\pi \sum_{J_f M_f} \sum_{l_0 l_f} \langle l_0 \mu_0 | S_f \nu_f | J_f M_f \rangle Y_{l_0 \mu_0}(\hat{\mathbf{t}}) R_{J_f, l_0 l_f}^{|t|}(r) i^{l_f} \mathcal{Y}_{1l_f}^{J_f M_f}(\hat{\mathbf{r}}) \mathcal{J}_{T_{23}\tau_{23}} \quad (\text{A3})$$

where $l_0, l_f = J_f \pm 1, J_f$. Note that the presence of tensor forces in the NN-potential leads to an admixture of partial waves with $l = J_f - 1$ and $l = J_f + 1$. This hinders the use of real phase shifts for the asymptotic behaviour of the radial functions $R_{J_f, l_0 l_f}^{|t|}(r)$ and, consequently, the Schrödinger equation cannot be solved in terms of real solutions. However, a unitary transformation V allows one to define new radial functions $\tilde{R} = VR$ which are eigenfunctions of the scattering problem, i.e., solutions of the Schrödinger equation with the proper asymptotic behaviour.

3. Wave function overlaps and the spectral function $P(|\mathbf{k}_1|, E)$ of 3He .

The Spectral function for the three-body break-up channel can be expressed in terms of the overlap between the three-body and two-body radial functions by substituting (A1)-(A3) into Eq. (24). Using the orthogonality of the spherical harmonics $Y_{lm}(\hat{\mathbf{t}})$ and the completeness of the Clebsch-Gordan coefficients, one obtains that only diagonal $(\{\alpha\} =$

$\{\alpha_N\}$) matrix elements contribute to the spectral function, viz.

$$\begin{aligned} P_{ex}(|\mathbf{k}_1|, E) &= \frac{1}{2} \sum_{M_{He}} \sum_{\sigma_f, S_f, \nu_f} \int \frac{d^3 \mathbf{t}}{(2\pi)^3} \left| \int d\boldsymbol{\rho} d\mathbf{r} \Psi_{He}(\boldsymbol{\rho}, \mathbf{r}) \Psi_{S_f \nu_f}^{\mathbf{t}}(\mathbf{r}) e^{-i\boldsymbol{\rho} \mathbf{k}_1} \right|^2 \delta \left(E_m - \frac{\mathbf{t}^2}{M_N} - E_3 \right) = \\ &= \frac{M_N \sqrt{M_N E_{rel}}}{2\pi^3} f_{iso} \sum_{\{\alpha\}} \left| \int \rho^2 d\rho j_{L_\rho}(p\rho) \mathcal{O}_{\{\alpha\}}^{E_{rel}}(\rho) \right|^2 \end{aligned} \quad (\text{A4})$$

where $f_{iso} = 3(1)$ for the pair in the isosinglet (isotriplet) final state, $j_{L_\rho}(p\rho)$ is the spherical Bessel functions, and the dimensionless overlap integrals $\mathcal{O}_{\{\alpha\}}^{E_{rel}}(\rho)$ are defined as follows

$$\mathcal{O}_{\{\alpha\}}^{E_{rel}}(\rho) = \int R_{\{\alpha\}}(r, \rho) \tilde{R}_{\{\alpha\}}^{|\mathbf{t}|}(r) r^2 dr \quad (\text{A5})$$

The normalization of the proton spectral function (A4)-(A5) is

$$\int d^3 \mathbf{k}_1 dE P(|\mathbf{k}_1|, E) \approx \begin{cases} 0.15 & \text{for } T_{23} = 0 \\ 0.50 & \text{for } T_{23} = 1 \end{cases} \quad (\text{A6})$$

so that the two-body break-up channel is normalized to ≈ 1.35 . Since the FSI factors S^{FSI} and S_{Δ}^{FSI} (Eqs. (77) and (80)) are no spherically symmetric, the distorted Spectral Function $P_{ex}^{FSI}(\mathbf{p}_m, E_m)$ (Eq. 76) is not longer diagonal with respect to the $(L_\rho, X, j_{23}, S_{23})$ configurations. Except for parity constraints (A2), any values of angular momenta of the pair in the final state contribute to $P_{ex}^{FSI}(\mathbf{p}_m, E_m)$.

APPENDIX B: FACTORIZATION OF THE COVARIANT CROSS SECTION

In this Appendix we will show, within a fully covariant approach, that under certain kinematical conditions the cross section for the process $A(e, e'p)X$ process factorizes even in presence of FSI. We shall consider, to this end, the deuteron (D) treated within the Bethe-Salpeter (BS) formalism. As mentioned, the factorization depends upon the spin structure of the square of the matrix element $[\bar{u}(\mathbf{k}_1, \tilde{s}_1) \Phi_D^{\mathcal{M}_2}(k_1, k_2) (\hat{k}_2 + M_N) v(\mathbf{k}_2, s_2)]$ appearing in Eq. (31) or, in case of FSI, upon the structure of $[\bar{u}(\mathbf{k}_1, \tilde{s}_1) \Phi_D^{\mathcal{M}_2}(k_1, k_2) v(\mathbf{k}_2, s_2)]$ (cf Eq. 40). The relevant spin parts can be evaluated directly by using the explicit form of the Dirac spinors, u and v , and the explicit expressions for the amplitudes $\Phi_D^{\mathcal{M}_2}(k_1, k_2)$ (cf., refs. [38, 39, 41]

1. Basic Definitions

In what follows the nucleon mass will be denoted by M_N , the mass of the deuteron by M_D and the mass of a generic nucleus A , by M_A . The Dirac spinors, with normalization

$\bar{u}(\mathbf{k}, s)u(\mathbf{k}, s) = 2M_N$, are

$$u(\mathbf{k}, s) = N_1 \begin{pmatrix} \chi_s \\ \frac{\sigma \mathbf{k}}{E_{\mathbf{k}} + M_N} \chi_s \end{pmatrix}; \quad v(\mathbf{k}, s) = N_1 \begin{pmatrix} \frac{\sigma \mathbf{k}}{E_{\mathbf{k}} + M_N} \tilde{\chi}_s \\ \tilde{\chi}_s \end{pmatrix}, \quad (B1)$$

where $k = (E_{\mathbf{k}}, \mathbf{k})$, $N_1 = \sqrt{E_{\mathbf{k}} + M_N}$, $E_{\mathbf{k}} = \sqrt{\mathbf{k}^2 + M_N^2}$ and $\tilde{\chi}_s \equiv -i\sigma_y \chi_s$.

The main Deuteron BS amplitudes, $\Phi_{^3S_1^{++}}$ and $\Phi_{^3D_1^{++}}$, corresponding to $L = 0$ and $L = 2$, respectively, have the following form

$$\Phi_{^3S_1^{++}}^{\mathcal{M}_2} = N(\hat{k}_1 + M_N) \frac{1 + \gamma_0}{2} \hat{\xi}_{\mathcal{M}_2}(\hat{k}_2 - M_N) \phi_S(k_0, |\mathbf{k}|) \quad (B2)$$

$$\begin{aligned} \Phi_{^3D_1^{++}}^{\mathcal{M}_2} = -\frac{N}{2}(\hat{k}_1 + M_N) \frac{1 + \gamma_0}{2} & \left(\hat{\xi}_{\mathcal{M}_2} + \frac{3}{2|\mathbf{k}|^2}(\hat{k}_1 - \hat{k}_2)(k \xi_{\mathcal{M}_2}) \right) \times \\ & \times (\hat{k}_2 - M_N) \phi_D(k_0, |\mathbf{k}|) \end{aligned} \quad (B3)$$

where \mathcal{M}_2 is the projection of the deuteron spin, $k_1 = (E_{\mathbf{k}}, \mathbf{k})$ $k_2 = (E_{\mathbf{k}}, -\mathbf{k})$, $k = (p_1 - p_2)/2$, $P_D = (p_1 + p_2) = (M_D, \mathbf{0})$, $N = \frac{1}{\sqrt{8\pi}} \frac{1}{2E_{\mathbf{k}}(E_{\mathbf{k}} + M_N)}$. The polarization vectors $\xi_{\mathcal{M}_2}$ are defined as follows

$$\xi_1 = -\frac{1}{\sqrt{2}} \begin{pmatrix} 0 \\ 1 \\ i \\ 0 \end{pmatrix}; \quad \xi_{-1} = \frac{1}{\sqrt{2}} \begin{pmatrix} 0 \\ 1 \\ -i \\ 0 \end{pmatrix}; \quad \xi_0 = \begin{pmatrix} 0 \\ 0 \\ 0 \\ 1 \end{pmatrix} \quad (B4)$$

and satisfy the well known relation

$$\sum_{\mathcal{M}_2} (\xi_{\mathcal{M}_2}^\mu \xi_{\mathcal{M}_2}^{+\nu}) = \left(-g^{\mu\nu} + \frac{P_D^\mu P_D^\nu}{M_D^2} \right) \quad (B5)$$

2. The PWIA

In Ref. [40] the Feynman diagrams for the process $D(e, e'p)X$ have been evaluated including all BS components. Here we re-calculate the diagrams for the $^3S_1^{++}$ and $^3D_1^{++}$ components in a slightly different manner which will be useful when FSI effects are considered.

In PWIA the cross section reads as follows

$$\frac{d\sigma}{dE' d\Omega'} = \sigma_{Mott} \tilde{l}^{\mu\nu} L_{\mu\nu}^D \frac{d^3 p_1}{(2\pi)^3 2E_1} \frac{d^3 p_2}{(2\pi)^3 2E_2} \quad (B6)$$

where $\tilde{l}^{\mu\nu}$ and $L_{\mu\nu}^D$ are the leptonic and hadronic tensors, respectively, the latter being

$$L_{\mu\nu}^D = \frac{1}{2M_D} \frac{1}{3} \sum_{\mathcal{M}_2, s_1, s_2} T_\mu(\mathcal{M}_2, s_1, s_2) T_\nu(\mathcal{M}_2, s_1, s_2) (2\pi)^3 \delta^{(4)}(P_D + q - p_1 - p_2) = \text{ (B7)}$$

$$= \langle \mathcal{M}_2 | \hat{J}_\mu^N | p_1, s_1, p_2, s_2 \rangle \langle p_1, s_1, p_2, s_2 | \hat{J}_\nu^N | \mathcal{M}_2 \rangle (2\pi)^3 \delta^{(4)}(P_D + q - p_1 - p_2) \quad \text{(B8)}$$

where \hat{J}_μ^N is the nucleon electromagnetic current operator. The amplitude T_μ could be written in the following form

$$T_\mu(\mathcal{M}_2, s_1, s_2) = \bar{u}(\mathbf{p}_1, s_1) \Gamma_\mu^{\gamma^* N}(Q^2, k_1^2) \Phi_D^{\mathcal{M}_2}(k_1, k_2) \tilde{S}^{-1}(\hat{k}_2) v(\mathbf{p}_2, s_2) \quad \text{(B9)}$$

where $\Phi_D^{\mathcal{M}_2}$ is a short-hand notation for the BS amplitudes (Eq. B3), $k_2 = p_2$, $S^{-1}(\hat{k}_2) = \hat{k}_2 + m$, and $\Gamma_\mu^{\gamma^* N}(Q^2, k_1^2)$ is the electromagnetic eN vertex which, for an off mass shell nucleon, depends not only upon Q^2 , but upon $k_1^2 \neq m^2$ as well.

By introducing between $\Gamma_\mu(Q^2, p_1, k_1)$ and $\Phi_D^{M_D}(k_1, k_2)$ the complete set of the Dirac spinors

$$\frac{1}{2M_N} \sum_{\tilde{s}_1} [u(\mathbf{k}_1, \tilde{s}_1) \bar{u}(\mathbf{k}_1, \tilde{s}_1) - v(\mathbf{k}_1, \tilde{s}_1) \bar{v}(\mathbf{k}_1, \tilde{s}_1)] \quad \text{(B10)}$$

and bearing in mind that for the $^3S_1^{++}$ and $^3D_1^{++}$ partial waves the second term in (B10) does not contribute, we obtain

$$\begin{aligned} T_\mu(\mathcal{M}_2, s_1, s_2) &= \frac{1}{2M_N} \sum_{\tilde{s}_1} J_\mu^{eN}(Q^2, p_1, k_1, \tilde{s}_1, s_1) \times \\ &\times \left[\bar{u}(\mathbf{k}_1, \tilde{s}_1) \Phi_D^M(k_1, k_2) \tilde{S}^{-1}(\hat{k}_2) v(\mathbf{p}_2, s_2) \right] \end{aligned} \quad \text{(B11)}$$

where $J_\mu^{eN}(Q^2, p_1, k_1) = \langle \mathbf{p}_1, s_1 | \Gamma_\mu^{\gamma^* N}(Q^2, k_1^2) | \mathbf{k}_1, \tilde{s}_1 \rangle$.

Let us evaluate Eq. (B11) for the D wave. One has

$$\begin{aligned} &\left[\bar{u}(\mathbf{k}_1, \tilde{s}_1) \Phi_{^3D_1^{++}}^{\mathcal{M}_2}(k_1, k_2) \tilde{S}^{-1}(\hat{k}_2) v(\mathbf{p}_2, s_2) \right] = \\ &= -\frac{NN_1^2}{\sqrt{2}} (k_2^2 - M_N^2) \phi_D(k_0, |\mathbf{k}|) 2m \left\langle \chi_{\tilde{s}_1}^\dagger \left| \left\{ -(\boldsymbol{\sigma} \boldsymbol{\xi}^M) + 3(\mathbf{n} \boldsymbol{\xi}^M)(\mathbf{n} \boldsymbol{\sigma}) \right\} \right| \tilde{\chi}_{s_2} \right\rangle \end{aligned} \quad \text{(B12)}$$

where \mathbf{n} is a unit vector along \mathbf{k} , i.e., $\mathbf{n} = \frac{\mathbf{k}}{|\mathbf{k}|} = \frac{\mathbf{k}_1}{|\mathbf{k}_1|}$. When Eq. (B12) is inserted in the expression for the cross section, one obtains

$$\begin{aligned} &\frac{1}{3} \sum_{\mathcal{M}_2, s_2} \left\langle \chi_{\tilde{s}_1} \left| \left\{ -(\boldsymbol{\sigma} \boldsymbol{\xi}^{\mathcal{M}_2}) + 3(\mathbf{n} \boldsymbol{\xi}^{\mathcal{M}_2})(\mathbf{n} \boldsymbol{\sigma}) \right\} \right| \tilde{\chi}_{s_2} \right\rangle \times \\ &\times \left\langle \tilde{\chi}_{s_2} \left| \left\{ -(\boldsymbol{\sigma} \boldsymbol{\xi}^{+\mathcal{M}_2}) + 3(\mathbf{n} \boldsymbol{\xi}^{+\mathcal{M}_2})(\mathbf{n} \boldsymbol{\sigma}) \right\} \right| \chi_{\tilde{s}_1} \right\rangle = 2\delta_{\tilde{s}_1 \tilde{s}_1'} \end{aligned} \quad \text{(B13)}$$

The last relation ensures factorization of the cross section; as a matter of fact, by performing the same procedure for the S -wave, it is easy to show that, thanks to Eq. (B13), the cross section (Eq. (B6)) factorizes, assuming the form (36) with n_D given by Eq. (34). In obtaining the above equations we expressed the BS amplitudes $\phi_L(k_0, |\mathbf{k}|)$ in terms of the BS vertices $G_{3L_1^{++}}(k_0, |\mathbf{k}|)$ and the radial functions u_L , by the relations

$$\frac{NN_1^2}{\sqrt{2}}(k_0^2 - M_N^2)\phi_D(k_0, |\mathbf{k}|) = \frac{NN_1^2 2E_{\mathbf{k}}}{\sqrt{2}} \frac{G_{3D_1^{++}}(k_0, |\mathbf{k}|)}{M_D - 2E_{\mathbf{k}}} \quad (\text{B14})$$

where $k_0 = \frac{M_D}{2} - E_{\mathbf{k}}$, and

$$u_{S(D)} = \frac{G_{3S_1^{++}(3D_1^{++})}(k_0, |\mathbf{k}|)/(4\pi)}{\sqrt{2M_D}(M_D - 2E_{\mathbf{k}})} \quad (\text{B15})$$

Note that in Eq. (B15) the normalization of the wave function is chosen so as to correspond to the non relativistic deuteron wave function

$$\frac{2}{\pi} \int |\mathbf{k}|^2 d|\mathbf{k}| (u_S^2(|\mathbf{k}|) + u_D^2(|\mathbf{k}|)) \approx 1 \quad (\text{B16})$$

We reiterate that factorization in PWIA occurs because the sum over s_2 and \mathcal{M}_2 of the square of the matrix element in Eq. (B13) becomes diagonal with respect to \tilde{s}_1 , i.e. because of Eq. (B13).

When FSI is taken into account, instead of Eq. (B13), one obtains for the D -wave (for the S -wave the spin structure is trivial)

$$\begin{aligned} & \frac{1}{3} \sum_{\mathcal{M}_2, s_2} \left[\bar{u}(\mathbf{k}_1, s_1) \Phi_D^{\mathcal{M}_2}(k_1, k_2) v(\mathbf{k}_2, s_2) \right]^\dagger \left[\bar{u}(\mathbf{k}'_1, \tilde{s}_1) \Phi_D^{\mathcal{M}_2}(k'_1, k'_2) v(\mathbf{k}'_2, s_2) \right] \simeq \\ & \frac{1}{3} \sum_{M, s_2} \left\langle \chi_{s_1} \left| \left\{ -(\boldsymbol{\sigma} \boldsymbol{\xi}^{\mathcal{M}_2}) + 3(\mathbf{n} \boldsymbol{\xi}^{\mathcal{M}_2})(\mathbf{n} \boldsymbol{\sigma}) \right\} \right| \tilde{\chi}_{s_2} \right\rangle \left\langle \tilde{\chi}_{s_2} \left| \left\{ -(\boldsymbol{\sigma} \boldsymbol{\xi}^{+M_2}) + 3(\mathbf{n}' \boldsymbol{\xi}^{+M_2})(\mathbf{n}' \boldsymbol{\sigma}) \right\} \right| \chi_{\tilde{s}_1} \right\rangle = \\ & = \frac{1}{3} \sum_{\mathcal{M}_2} \left\langle \chi_{s_1} \left| \left\{ -(\boldsymbol{\sigma} \boldsymbol{\xi}^{\mathcal{M}_2}) + 3(\mathbf{n} \boldsymbol{\xi}^{\mathcal{M}_2})(\mathbf{n} \boldsymbol{\sigma}) \right\} \left\{ -(\boldsymbol{\sigma} \boldsymbol{\xi}^{+M_2}) + 3(\mathbf{n}' \boldsymbol{\xi}^{+M_2})(\mathbf{n}' \boldsymbol{\sigma}) \right\} \right| \chi_{\tilde{s}_1} \right\rangle \end{aligned} \quad (\text{B17})$$

where \mathbf{n} (\mathbf{n}') is a unit vector along \mathbf{k}_1 (\mathbf{k}'_2).

By taking into account the completeness of the polarization vectors $\boldsymbol{\xi}$, the only spin dependence remaining in Eq. (B17) is contained in the term

$$\frac{1}{3} \sum_M (\mathbf{n} \boldsymbol{\xi}^M)(\mathbf{n} \boldsymbol{\sigma})(\mathbf{n}' \boldsymbol{\xi}^{+M})(\mathbf{n}' \boldsymbol{\sigma}) = (\mathbf{n} \mathbf{n}') \left((\mathbf{n} \mathbf{n}') - i \boldsymbol{\sigma} [\mathbf{n} \times \mathbf{n}'] \right), \quad (\text{B18})$$

so that in case of rescattering with low momentum transfer, when in the integral over \mathbf{k}_2 the main contribution comes from $\mathbf{k}_2 \sim \mathbf{p}_2, \mathbf{k}'_2 \sim \mathbf{p}_2$, one has $\sigma[\mathbf{n} \times \mathbf{n}'] = 0$ and factorization is approximately recovered, with the S and D waves adding incoherently.

Thus, to sum up, factorization is compatible with FSI if:

1. The spin-flip part of the NN amplitude should be very small, as it occurs when either the 3-momentum transfers \mathbf{q} , or the momentum of the $|\mathbf{p}_1|$ are large;
2. the momentum transfer κ in the NN rescattering has to be small so that in the integral $\mathbf{k}_2 \sim \mathbf{p}_2$. This appears to be the case since the NN amplitude is sharply peaked forward.
3. The contribution from $N\bar{N}$ pair currents can be neglected, which is ensured by the smallness of the P wave in the deuteron.

- [1] W. Glöckle *et al*, Phys. Rep. **274** (1996) 107.
- [2] A. Kievsky, S. Rosati and M. Viviani, Nucl. Phys. **A551** (1993) 241 and *Private communication*.
- [3] S. C. Pieper, R. B. Wiringa, Ann. Rev. Nucl. Part. Sci. **51**, (2001) 53.
- [4] S.C. Pieper, R.B. Wiringa and V.R. Pandharipande, Phys. Rev. **C46**, 1741 (2000).
- [5] R. B. Wiringa, V. G. J. Stoks and R. Schiavilla, Phys. Rev. **C51** (1995) 38.
- [6] V.N.Gribov, Sov. Phys. JETP, **30** (1970) 709.
- [7] L. Bertocchi, Nuovo Cimento, **11A** (1972) 45.
- [8] J. H. Weis, Acta Phys. Pol. **B7**(1976)851.
- [9] L.L. Frankfurt, W.R. Greenberg, G.A. Miller, M.M. Sargsian, M.I. Strikman, Z. Phys. **A352** (1995) 97.
- [10] L.L. Frankfurt, M.M. Sargsian, M.I. Strikman, Phys. Rev. **C56** (1997) 1124.
- [11] M.M. Sargsian, Int. J. Mod. Phys. **E10**(2001)405.
- [12] M.A. Braun, C.Ciofi degli Atti, D. Treleani, Phys. Rev. **C62**, 034606 (2000).
- [13] M. Braun, Ciofi degli Atti, L.P. Kaptari, Eur. J. Phys. **A19** (2004)143
nucl-th/0311060.
- [14] H. Morita, M. Braun, C. Ciofi degli Atti and D. Treleani Nucl.Phys. **A699** (2002) 328.

- [15] R. J. Glauber, in *Lectures in Theoretical Physics*, W. E. Brittin *et al* Editors, New York (1959).
- [16] W. -J. Kasdorp, W. H. A. Hessenlik, D. Groep, E. Jans, *et al*, Few Body Systems **25**(1998)115.
- [17] P.E. Ulmer, K.A. Aniol, H. Arenhövel, J.-P. Chen, *et al*. Phys. Rev. Lett., **89** (2002) 062301-1.
- [18] H.J. Bulten, P.L. Anthony, R.G. Arnold, E.J. Beise, Phys. Rev. Lett., **74** (1995) 4775.
- [19] C. Marchand, M. Bernheim, P. C. Dunn, A. Gérard, *et al*, Phys. Rev. Lett. **60** (1988) 1703.
- [20] A. Saha, M. Epstein, E. Voutier (*spokespersons*), Jlab Experiment E-89-044 and *Private communication*.
- [21] D. W. Higinbotham, *for the Jefferson Lab Hall A Collaboration*, Eur. Phys. Jou. **A19**(2004)171.
- [22] C.Ciofi degli Atti and L.P. Kaptari, invited paper at *International Workshop on Probing Nucleons and Nuclei via the $(e, e'p)$ reaction*, 14-17 october 2003, Grenoble (France); nucl-th/0312043.
- [23] M. Alvioli, C. Ciofi degli Atti, L.P. Kaptari, H. Morita Proceedings of the *6th Workshop on Electromagnetically induced Two Hadron Emission*, Pavia, Italy, 24-27 Sep 2003, nucl-th/0312123.
- [24] S. Boffi, C. Giusti and F.D. Pacati, Phys. Rep. **226** (1993). 1.
- [25] R. -W. Schulze and P. E. Sauer, Phys. Rev. **C226** (1993)38.
- [26] C. Ciofi degli Atti, E. Pace and G. Salmè, Phys. Rev. **21** (1980) 805.
- [27] A. Kievski, E. Pace, G. Salmè and M. Viviani, Phys. Rev. **C56**(1997)64.
- [28] C. Ciofi degli Atti, E. Pace and G. Salmè in *Lecture Notes in Physics* **86** (1978) 315;
- [29] H. Meier-Hadjuk, Ch. Hadjuk, P. E. Sauer and W. Thies, Nucl. Phys. **A395** (1983) 342.
U. Oelfke, P. U. Sauer and F. Coester, Nucl. Phys. **A518** (1990)593.
- [30] C. Ciofi degli Atti, L. Kaptari and S. Scopetta, Eur. Phys. Jou. **A5** (1999) 191
- [31] T. de Forest Jr., Nucl. Phys. **A392** (1983) 232.
- [32] R.V. Reid Jr., Ann. Phys. **50** (1968) 411.
- [33] L. L. Frankfurt and M.I. Strikman, Phys. Rep. **160** (1988) 235.
- [34] C. Ciofi degli Atti, S. Simula, L.L. Frankfurt and M.I. Strikman, Phys. Rev. C 44 (1991) R7;
C. Ciofi degli Atti and S. Simula, Phys. Rev. **C53** (1996) 1689.
- [35] J. Golak, H. Witala, R. Skininski, W. Glöckle, A. Nogga, H. Kamada nucl-th/0403022 (2004).
- [36] C. Ciofi degli Atti, L. P. Kaptari, Phys. Rev. **C66** (2002)044004.
- [37] S. Jeschonnek, Phys. Rev. **C63** (2001) 034609.

[38] B.D. Keister, J.A. Tjon, Phys. Rev. **C 26** (1982) 578;
 G. Rupp, J.A. Tjon, Phys. Rev. **C 41** (1990) 472;
 J.J. Kubis, Phys. Rev. **D 6** (1972) 547;
 M.J. Zuilhof, J.A. Tjon, Phys. Rev. **C 22** (1980) 2369.

[39] F. Gross, Phys. Rev. **185** (1969) 1448;
 W.W. Buck, F. Gross, Phys. Rev. **C 20** (1979) 2361;
 F. Gross, J.V. Van Orden, K. Holinde, Phys. Rev. **C 45** (1992) 2094.

[40] C. Ciofi degli Atti, D. Faralli, A.Yu. Umnikov and L.P. Kaptari, Phys. Rev. **C60** (1999) 034003.

[41] L.P. Kaptari, B. Kampfer, S.M. Dorkin, S.S. Semikh, Few Body Syst. **27** (1999) 189;
 L.P. Kaptari, B. Kampfer, S.M. Dorkin, S.S. Semikh, Phys.Rev. **C 57** (1998) 1097.

[42] C. Ciofi degli Atti, L.P. Kaptari and D. Treleani Phys. Rev. **C63** (2001) 044601.

[43] N. N. Nikolaev, J. Speth, B. G. Zakharov, JETP **82**, (1996) 1046;
 nucl-th/9501016.

[44] A. Bianconi, S. Jeschonnek, N. N. Nikolaev and B. G. Zacharov, Phys. Lett. **A343** (1995)13.

[45] R.A. Arndt *et al*, "(SAID) Partial-Wave Analysis Facility", <http://said.phys.vt.edu/>.

[46] H. Morita, C.Ciofi degli Atti and D. Treleani, Phys. Rev. **C60**(1999) 34603-1.

[47] F. Ritz, H. Göller, T. Wilbois and H. Arenhövel, Phys. Rev. **C55**(1997)2214.

[48] G. Beck and H. Arenhövel, Few-Body Systems **13**(1992)165.

[49] G. Beck, T. Wilbois and H. Arenhövel, Few-Body Systems **17**(1994)91.

[50] J.-M. Laget, Phys. Lett. **B199**(1987)1046.

[51] J.-M. Laget, Phys. Rev. **D579**(1994)333.

[52] J.-M. Laget, in *New Vistas in Electronuclear Physics*, edited by E. Tomusiak *et al*, Plenum N.Y.,1986, p.361.

[53] J.-M. Laget, Few-Body Systems, Suppl. **0**(2004)1.
 nucl-th/0303052

[54] M. Alvioli, C. Ciofi degli Atti, L. Kaptari and H. Morita, *in preparation*.

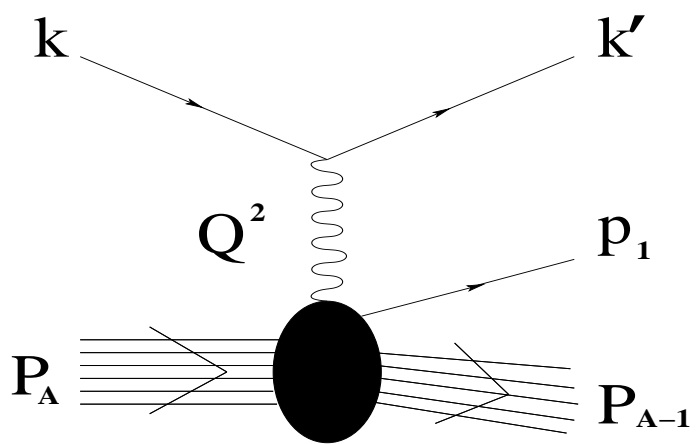
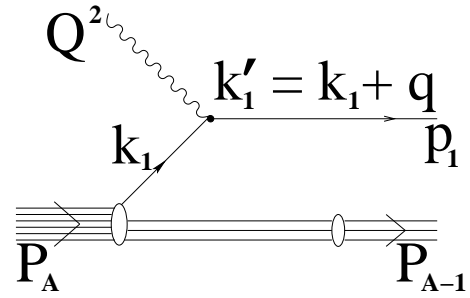
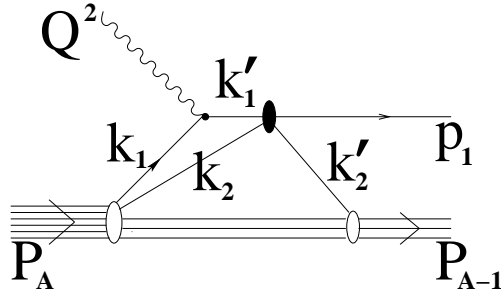


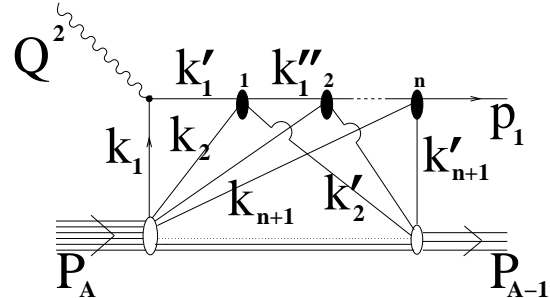
FIG. 1: The Feynman diagram describing the one-photon exchange approximation for the process $A(e, e'p)(A - 1)$.



a)



b)



c)

FIG. 2: The Feynman diagrams describing the Plane Wave Impulse Approximation (PWIA) (2a)), the single rescattering approximation (2b)), and the full $A - 1$ rescattering approximation (2c)), for the process $A(e, e'p)(A - 1)$. The four-momenta of particle i before and after rescattering is denoted by k_i , k'_i , k''_i , etc., respectively. The black oval spots denote the elastic nucleon-nucleon (NN) scattering matrix f^{NN} .

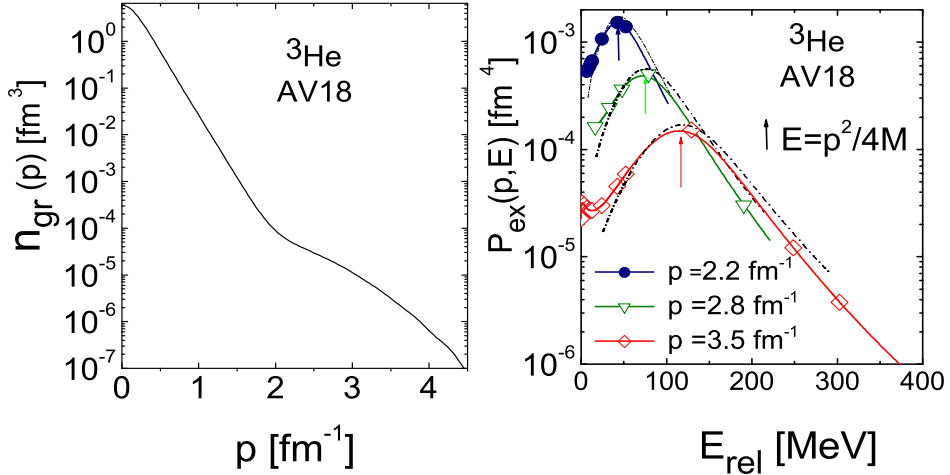


FIG. 3: The proton Spectral Function of ${}^3\text{He}$ (Eq.(21)). *Left panel:* n_{gr} (Eq. (23)) *vs* $p \equiv |\mathbf{k}_1|$. *Right panel:* P_{ex} (Eq. (24)) *vs* the excitation energy of the two-nucleon system in the continuum $E_{rel} = \frac{\mathbf{t}^2}{M_N} = E_2^f = E - E_{min}$, for various values of $p \equiv |\mathbf{k}_1|$. The dot-dashed curves represent the Plane Wave Approximation (PWA), when the three particles in the continuum are described by plane waves, whereas the full curves correspond to the PWIA, when the interaction in the spectator proton-neutron pair is taken into account. The arrows indicate the position of the peak ($\sim p^2/4M_N$) predicted by the two-nucleon correlation model for the Spectral Function [34] (three-body wave function from Ref. [2], AV18 interaction [5]).

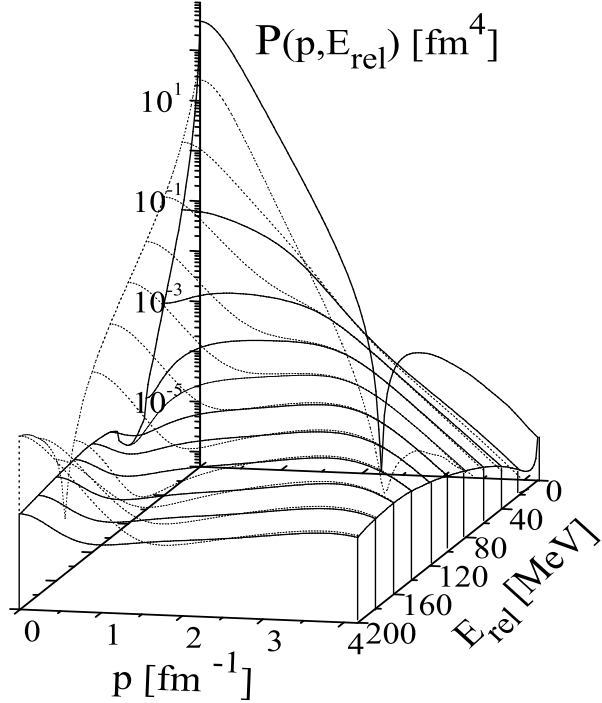
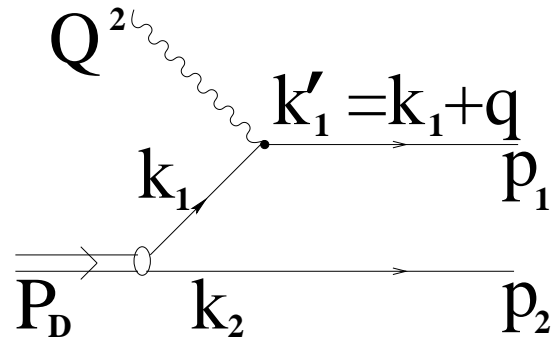
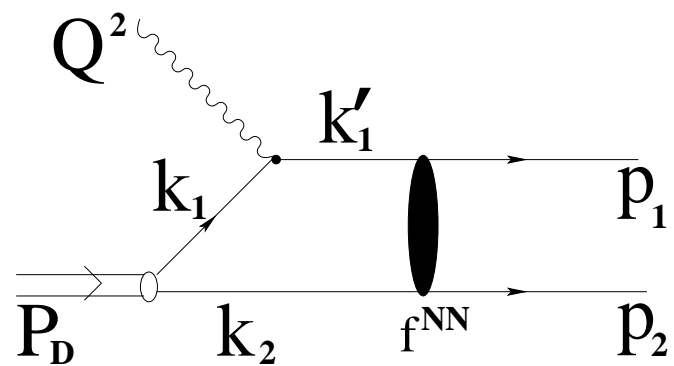


FIG. 4: The neutron Spectral Function of 3He (Eq. (24)) *vs* $p \equiv |\mathbf{k}_1|$ and the excitation energy of the two-nucleon system in the continuum $E_{rel} = \frac{t^2}{M_N} = E_2^f = E - E_{min}$. The dotted curves represent the *PWA*, when the three particles in the continuum are described by plane waves, whereas the full curves correspond to the *PWIA*, when the interaction in the spectator proton-proton pair is taken into account (three-body wave function from Ref. [2], *AV18* interaction [5]).

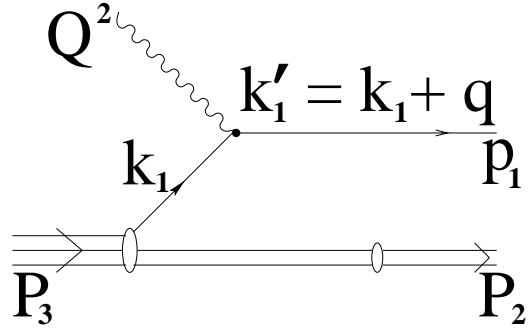


a)

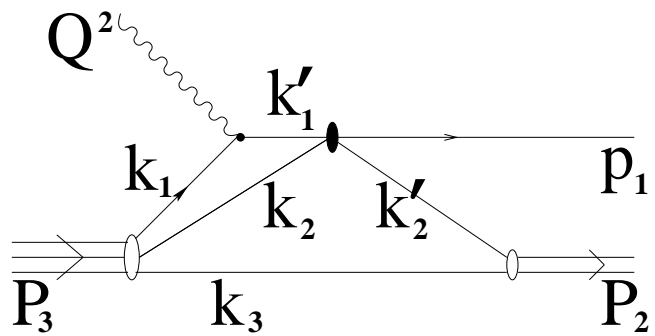


b)

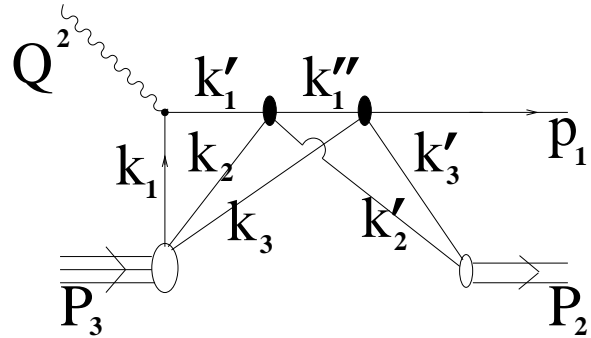
FIG. 5: The Feynman diagrams for the process ${}^2H(e, e'p)n$ representing the PWIA) (a)), and the single (b)) rescattering in the final state. f^{NN} denotes the elastic NN scattering amplitude



a)



b)



c)

FIG. 6: The Feynman diagrams representing the PWIA (a)), the single (b)), and double (c)) rescattering in the processes $^3He(e, e'p)D$ and $^3He(e, e'p)(np)$. In the former case the final two-nucleon state is a deuteron with momentum $\mathbf{P}_D = \mathbf{p}_2$, whereas in the latter case the final state represents two free nucleons with momenta \mathbf{p}_2 and \mathbf{p}_3 , with $\mathbf{P}_2 = \mathbf{p}_2 + \mathbf{p}_3$. The trivial single and double rescattering diagrams with nucleons "2" and "3" interchanged are not drawn. The black oval spots denote the elastic nucleon-nucleon (NN) scattering matrix f^{NN} .

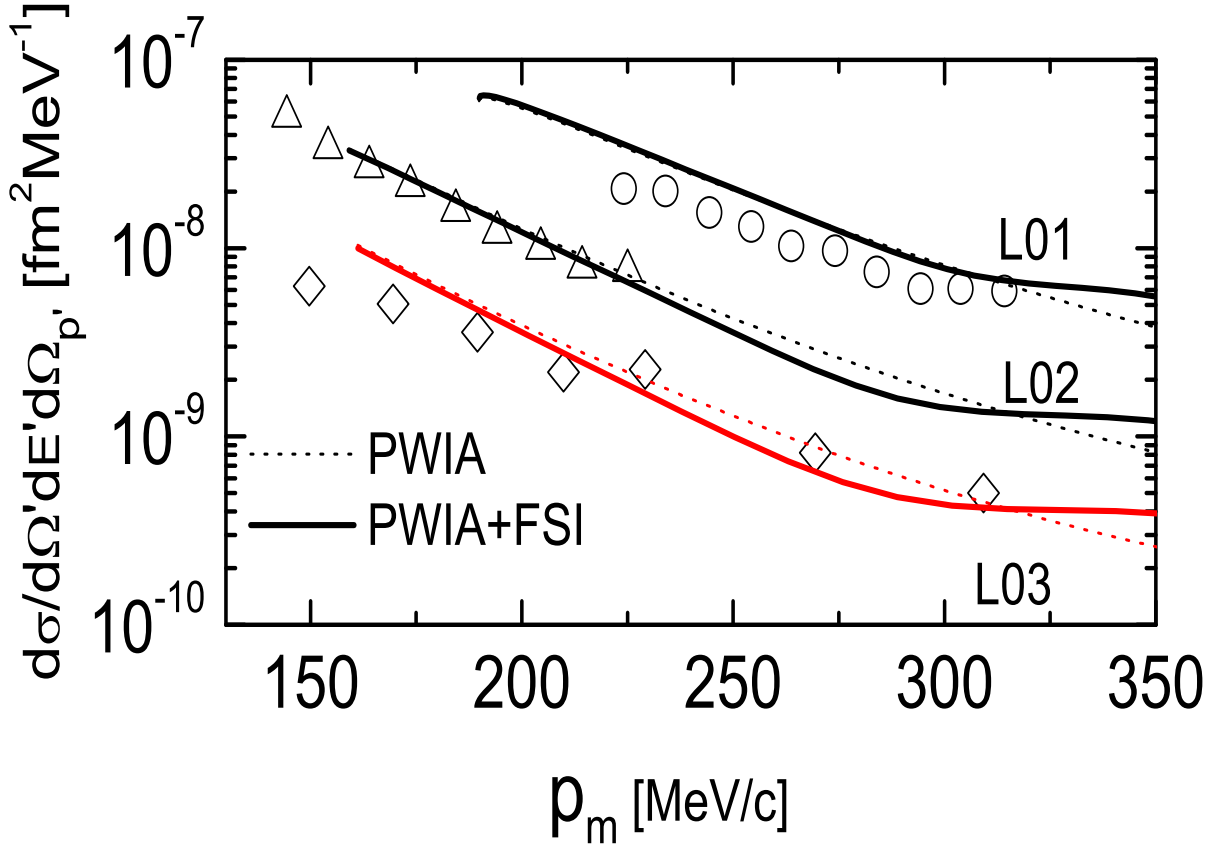


FIG. 7: The process $^2H(e, e'p)n$: the NIKHEF experimental data [16] *vs* the missing momentum $p_m \equiv |\mathbf{p}_m|$ are compared with our theoretical calculations; the dotted line represents the *PWIA*, whereas the full line include the final state rescattering. The curves labelled *L01*, *L02*, and *L03*, correspond to $Q^2 = 0.1$, 0.2 , and 0.3 (GeV/c^2), respectively, and $x \simeq 0.3 - 0.6$ (in this Figure and in Figs. 8-12, $p' \equiv |\mathbf{p}_1|$).

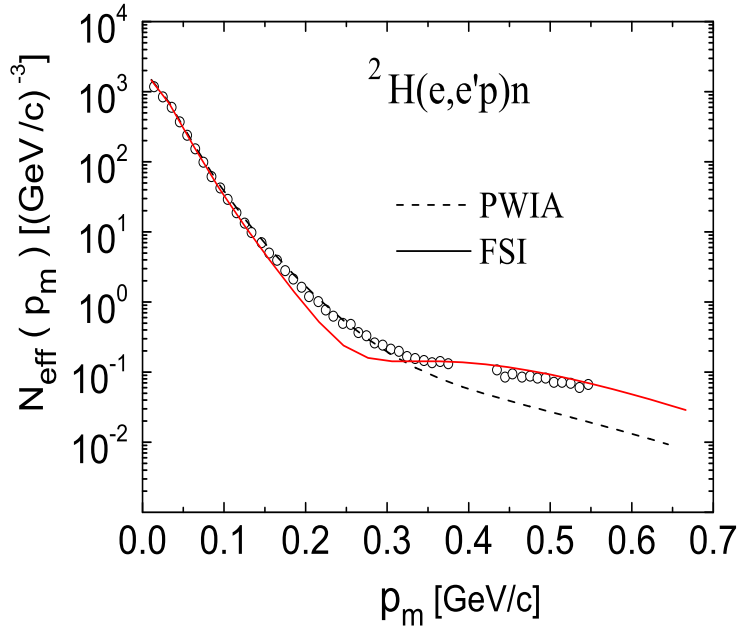


FIG. 8: The process ${}^2H(e, e'p)n$: the Jlab experimental data [17] (N_{eff} defined by Eq. (84)) *vs* the missing momentum $p_m \equiv |\mathbf{p}_m|$, compared with our theoretical calculations . The dotted line represents the PWIA whereas the full line includes the final state rescattering. The experimental data correspond to the perpendicular kinematics, with $Q^2 \simeq 0.665$ (GeV/c) 2 , $|\mathbf{q}| \simeq 0.7$ GeV/c , and $x \simeq 0.96$.

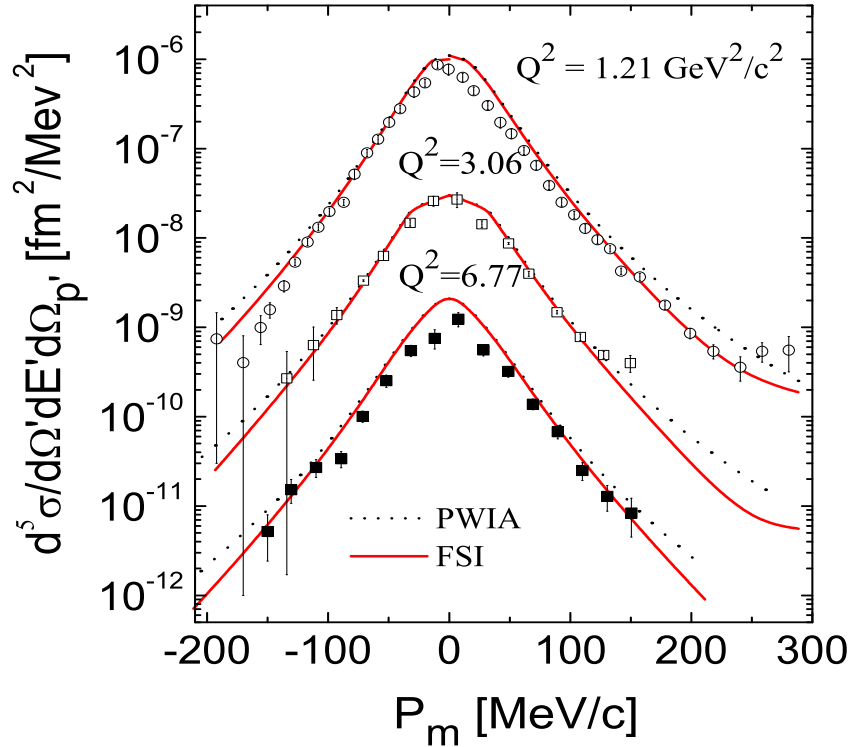


FIG. 9: The process $^2H(e, e'p)n$: the SLAC experimental data at $x \simeq 1$ [18] *vs* the missing momentum $p_m \equiv |\mathbf{p}_m|$, compared with our theoretical calculations. The dotted lines represent the PWIA and the full lines include the final state rescattering. The positive and negative values of p_m correspond to values of the azimuthal angle $\phi = \pi$ and 0, respectively.

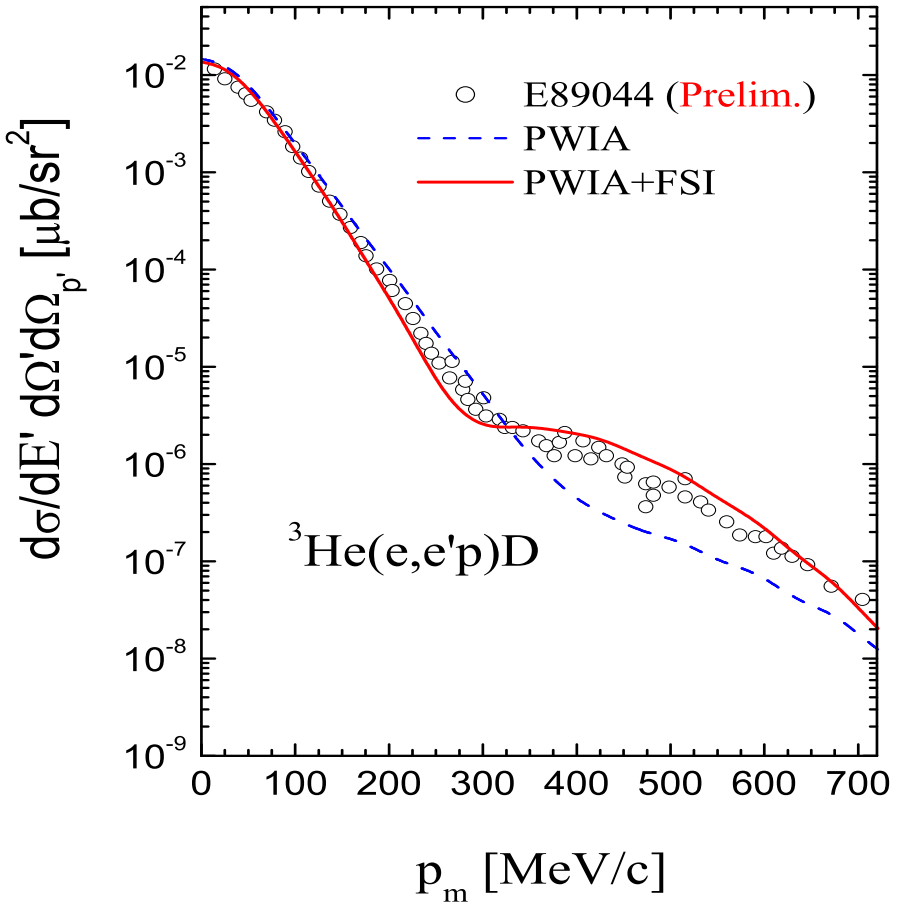


FIG. 10: The process ${}^3He(e, e'p)D$: the preliminary experimental data from JLab (JLab Experiment E-89-044 [20, 21]) *vs* $p_m \equiv |\mathbf{p}_m|$ compared, at $Q^2 = 1.55$ (GeV/c^2) and $x = 1$, with our theoretical results. The dashed line corresponds to the PWIA and the full line includes the full FSI calculated using Eq. (75); the predictions by Eq.(77) (GGA) and Eq. (80) (GA), differ by at most 4% and cannot be distinguished in the Figure (three-body wave function from [2], *AV18* interaction [5]).

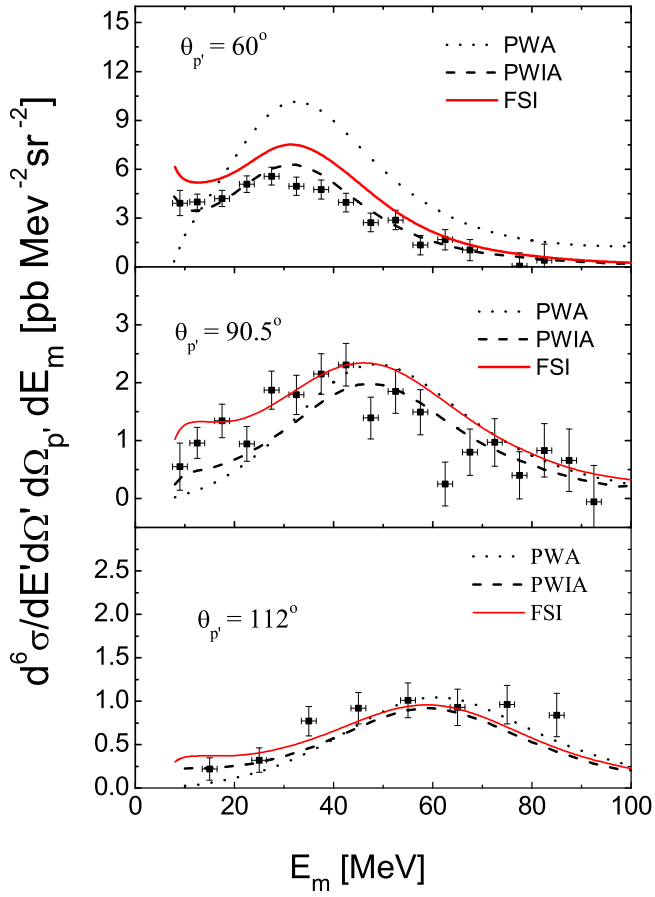


FIG. 11: The process $^3He(e, e'p)(np)$: the experimental data from Saclay [19] *vs* E_m for various values of the proton emission angle $\theta_{p'}$ ($p' \equiv |\mathbf{p}_1|$), compared with our theoretical results. The dotted lines correspond to the PWA, when the three nucleons in the final state are described by plane waves, the dashed lines correspond to the PWIA, when the interaction in the spectator neutron-proton pair is taken into account, and the full lines include the full FSI calculated using Eq. (75); the predictions by Eq.(77) (GGA) and Eq. (80) (GA), differ by at most 4% and cannot be distinguished in the Figure. Note that the values of the experimental p_m and E_m corresponding to the maxima of the cross section, satisfy to a large extent the relation predicted by the two-nucleon correlation mechanism [34], namely $E_m \simeq p_m^2/4M_N$ (cf. Fig. 3, right panel), with the full FSI mainly affecting only the magnitude of the cross section (three-body wave function from [2], *AV18* interaction [5]).

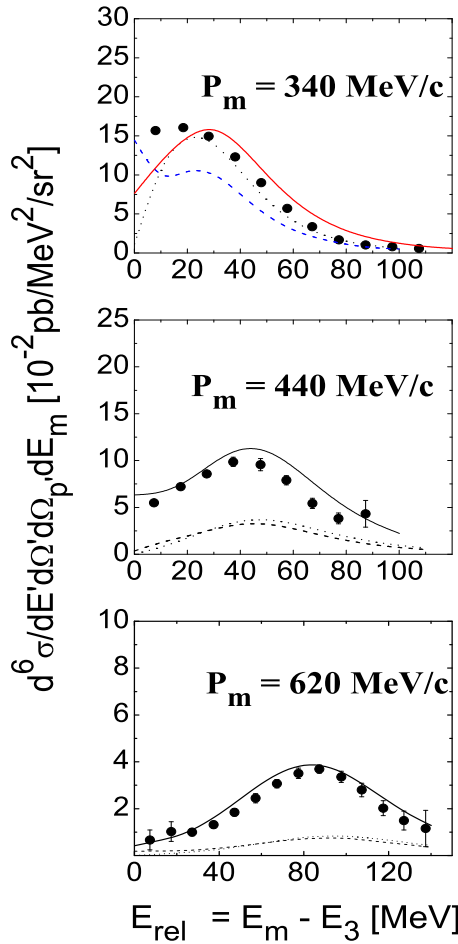


FIG. 12: The process $^3He(e, e'p)(np)$: the preliminary experimental data from JLab (JLab Experiment E-89-044 [20, 21]) at $Q^2 = 1.55$ (GeV/c^2) and $x = 1$, vs the excitation energy of the two-nucleon system in the continuum $E_{rel} = \frac{t^2}{M_N} = E_2^f = E_m - E_3$, compared with our theoretical results. The dotted lines correspond to the PWA, when the three nucleons in the final state are described by plane waves, the dashed line correspond to the PWIA, when the interaction in the spectator neutron-proton pair is taken into account, and the full line includes the full FSI calculated using Eq. (75); the predictions by Eq.(77) (GGA) and Eq. (80) (GA), differ by at most 4% and cannot be distinguished in the Figure. Note that the value of $p_m \equiv |\mathbf{p}_m|$ appearing in each inset corresponds to the maximum of the cross section; the experimental values of p_m and E_m at the maximum value of the cross section satisfy to a large extent the relation predicted by the two-nucleon correlation mechanism [34], namely $E_{rel} \simeq p_m^2/4M_N$ (cf. Fig. 3, right panel) (three-body wave function from [2], AV18 interaction [5]).